Biochemical Properties and Subcellular Distribution of the BI and rbA Isoforms of α_{1A} Subunits of Brain Calcium Channels

Takashi Sakurai, Ruth E. Westenbroek, Jens Rettig, Johannes Hell, and William A. Catterall

Department of Pharmacology, Mailbox 357280, University of Washington, Seattle, Washington 98195-7280

Abstract. Biochemical properties and subcellular distribution of the class A calcium channel $\alpha 1$ subunits (α_{1A}) from rat and rabbit brain were examined using site-directed anti-peptide antibodies specific for rat rbA (anti-CNA3) and for rabbit BI (anti–NBI-1 and anti–NBI-2) isoforms of α_{1A}. In immunoblotting experiments, anti-CNA3 specifically identifies multiple α_{1A} polypeptides with apparent molecular masses of 210, 190, and 160 kD, and anti–NBI-1 and anti–NBI-2 specifically recognize 190-kD α_{1A} polypeptides in rat brain membrane. In rabbit brain, anti–NBI-1 or anti–NBI-2 specifically detect α_{1A} polypeptides with apparent molecular masses of 220, 200, and 190 kD, while anti-CNA3 specifically recognizes 190-kD α_{1A} polypeptides. These polypeptides evidently represent multiple isoforms of α_{1A} present in both rat and rabbit brain. Anti-CNA3 specifically immunoprecipitates high affinity receptor sites for ω-conotoxin MVIIC ($K_d \sim 100$ pM), whereas anti–NBI-2 immunoprecipitates two distinct affinity receptor sites for ω-conotoxin MVIIC ($K_d \sim 100$ pM and ~ 1 μM). Coimmunoprecipitation experiments indicate that α_{1A} subunits recognized by anti-CNA3 and anti–NBI-2 are associated with syntaxin in a stable, SDS-resistant complex and with synaptotagmin. Immunofluorescence studies reveal that calcium channels recognized by anti–NBI-2 are localized predominantly in dendrites and nerve terminals forming synapses on them, while calcium channels recognized by anti-CNA3 are localized more prominently in cell bodies and in nerve terminals. The mossy fiber terminals in hippocampus and the terminals of climbing and parallel fibers in cerebellum are differentially stained by these isoform-specific antibodies. These results indicate that both rbA and BI isoforms of α_{1A} are expressed in rat and rabbit brain and form calcium channels having α_{1A} subunits with distinct molecular mass, pharmacology, and subcellular localization.

MULTIPLE types of voltage-dependent calcium channels have been distinguished on the basis of biophysical and pharmacological criteria (L, T, N, P, and Q) and may differ in their cellular distribution and functional roles (Llinas et al., 1989; Zhang et al., 1993). Voltage-dependent calcium channels are composed of five subunits ($\alpha 1$, $\alpha 2$, δ, β, and γ) (Catterall, 1988). The $\alpha 1$ subunit forms the ion-conducting pore and serves as a voltage sensor, while the other subunits can modulate calcium currents conducted by $\alpha 1$ (for review see Isom et al., 1994). Homology screening has led to the identification of five distinct classes of calcium channel $\alpha 1$ subunit in the rat brain, designated rbA, rbB, rbC, rbD, and rbE (Snutch

et al., 1990; Snutch and Reiner, 1992; Birnbaumer et al., 1994).

Both α_{1A} (α_1 subunit of class A brain calcium channel) and α_{1B} (α_1 subunit of class B brain calcium channel) subunits have been implicated in synaptic transmission. α_{1B} forms an N-type calcium channel that is neuro-specific and sensitive to the cone snail toxin ω-conotoxin GVIA (Dubel et al., 1992; Williams et al., 1992; Fujita et al., 1993). Class B N-type calcium channels are localized at high density in presynaptic terminals and at lower density in dendrites of central neurons (Westenbroek et al., 1992, 1995), and ω-conotoxin GVIA inhibits synaptic neurotransmission at the central and peripheral synapses (Horne and Kemp, 1991; Luebke et al., 1993; Wheeler et al., 1994; for review see Olivera et al., 1994; Dunlap et al., 1995), indicating that presynaptic N-type calcium channels are involved in synaptic exocytosis.

α_{1A} forms high-voltage–activated calcium channels expressed abundantly in the cerebellum including the Purkinje neurons (Mori et al., 1991; Starr et al., 1991; Sather et al., 1993; Stea et al., 1994), where P-type calcium current was first recorded (Llinas et al., 1989). ω-agatoxin IVA from venom of the funnel web spider *Agelenopsis aperta* and ω-conotoxin MVIIC from venom of the cone snail *Conus*

magus inhibit both P-type and Q-type calcium currents, but ω-agatoxin IVA has higher affinity for block of P-type currents, and ω-CTx-MVIIC has higher affinity for block of Q-type currents (Olivera et al., 1994). Calcium channels expressed in *Xenopus* oocytes from α_{1A} cDNA have the pharmacological characteristics of Q-type (Hillyard et al., 1992; Sather et al., 1993; Stea et al., 1994; Zhang et al., 1993; Randall et al., 1995). However, similarities in physiological properties and localization of α_{1A} subunits and P-type calcium channels suggest that specific isoforms of α_{1A} subunits may form both P-type and Q-type calcium channels (Mori et al., 1991; Sather et al., 1993; Stea et al., 1994; Westenbroek et al., 1995; DeWaard and Campbell, 1995).

Calcium channels containing α_{1A} subunits are widely distributed in the central nervous system and are localized in high density in the presynaptic nerve terminals of many classes of neurons and at lower density in dendrites (Ousley and Froehner, 1994; Westenbroek et al., 1993, 1995). ω-Agatoxin IVA and ω-conotoxin MVIIC inhibit excitatory glutamatergic transmission in the hippocampus (Takahashi and Momiyama, 1993; Luebke et al., 1993; Castillo et al., 1994; Wu and Saggau, 1994; Wheeler et al., 1994), inhibitory GABAergic neurotransmission in the cerebellum and spinal cord (Takahashi and Momiyama, 1993; Regehr and Mintz, 1994), and cholinergic transmission at neuromuscular junction (Uchitel et al., 1992; Bowersox et al., 1995). The inhibition of synaptic transmission by ω-agatoxin IVA occurs with distinct IC_{50} values in some presynaptic nerve terminals (Castillo et al., 1994). These results implicate P/Q-type calcium channels in synaptic neurotransmission at various synapses in the central and peripheral nervous system. They may be functionally more divergent and quantitatively more important than N-type channels in regulating calcium entry in the presynaptic nerve terminal (Dunlap et al., 1995).

Although calcium channels containing α_{1A} subunits appear to have diverse functional properties and important physiological roles, little is known about the molecular basis of diversity in α_{1A} subunits. cDNAs encoding α_{1A} subunits have been cloned from two different species, rabbit (BI; Mori et al., 1991) and rat (rbA; Starr et al., 1991). They share an overall amino acid sequence identity of 92%, but the intracellular loop between domains II and III (L_{II-III}) is strikingly divergent (78% identical) compared to the remainder of the protein (>98% identical in all other regions except the COOH-terminal region). This striking difference in conservation suggests that the BI and rbA cDNAs may encode isoforms with alternatively spliced sequences in L_{II-III}. cDNAs encoding multiple isoforms of α_{1A} have been reported for both BI and rbA (Mori et al., 1991; Starr et al., 1991; Stea et al., 1994), and we have identified multiple isoforms of the α_{1A} protein with different molecular masses that appear to arise from alternative mRNA splicing (Sakurai et al., 1995). However, it has not been determined whether both the rbA and BI isoforms are expressed in a single species. To examine whether the BI and rbA isoforms of α_{1A} are both expressed in a single species and may serve distinct functional roles, we detected the rbA and BI isoforms of α_{1A} subunits in rat and rabbit brain using specific site-directed anti-peptide antibodies and characterized their biochemical and pharmacological properties and their subcellular distribution.

Materials and Methods

Materials

[3H]isradipine (PN200-110; 80 Ci/mmol) and [125I]ω-conotoxin GVIA (2,200 Ci/mmol) were purchased from Dupont-New England Nuclear (Wilmington, DE). [125I]ω-conotoxin MVIIC was a generous gift from Drs. A. Woppmann, L. Nadasi, and G.P. Miljanich of Neurex Corp. (Menlo Park, CA). Tricine precast gel was obtained from Novex™ (San Diego, CA), enhanced chemiluminescence (ECL) detection kit for immunoblotting from Amersham Corp. (Arlington Heights, IL), digitonin from Gallard-Schlesinger Chemical Mfg. Corp. (Carle Place, NY), and protein A–Sepharose (PAS)[1] and heparin-agarose from Sigma Chemical Co. (St. Louis, MO). Expression vector pGEX-4T and glutathione–Sepharose 4B were obtained from Pharmacia LKB Biotechnology (Piscataway, NJ). All other reagents were of standard biochemical quality from commercial sources. Monoclonal anti-syntaxin and anti-synaptotagmin antibodies, designated mAb10H5 and mAb1D12, respectively, were generous gifts from Dr. Masami Takahashi, Mitsubishi-Kasei Life Science Institute, Tokyo, Japan (Yoshida et al., 1992; Lévèque et al., 1992).

Production and Purification of Peptides and Anti-peptide Antibodies

The peptide CNA3 ([KY]SEPQQREHAPPREHV) corresponds to residues 882–896 and the peptide CNA1 ([KY]PSSPERAPGREGPYGRE) corresponds to residues 865–881 of rbA isolated from rat brain (Starr et al., 1991; Sakurai et al., 1995; Westenbroek et al., 1995). The peptide NBI-1 ([KY]TVDQRLGQQRAEDFLRK) and the peptide NBI-2 ([KY]SDH QAREGGLEPPGF) correspond to the residues 845–861, and 904–918 of BI derived from rabbit brain, respectively (Mori et al., 1991). These four peptide sequences are located in a highly variable segment in the intracellular loop between domains II and III of the α_{1A} subunit of brain calcium channels. The NH_2-terminal lysine and tyrosine are not part of the channel sequence and were added for cross-linking and labeling purposes. The CNA1, CNA3, NBI-1, and NBI-2 peptides were synthesized by the solid phase method (Merrifield, 1963), and then purified by reversed-phase high pressure liquid chromatography on a Vydac 281TP10 column (Hesperia, CA). The identities of the purified peptides were confirmed by amino acid analysis. The purified peptides were coupled through amino groups with glutaraldehyde to BSA, dialyzed against PBS, and emulsified in an equal volume of Freund's complete (initial injection) or incomplete adjuvant. The coupled peptides were injected into multiple subcutaneous sites on New Zealand White rabbits at 3-wk intervals. Antisera were collected after the second injection and tested by enzyme-linked immunosorbent assay using microtiter plates with wells coated with 0.5 μg of peptide (Posnett et al., 1988). Antibodies were purified by affinity chromatography on the corresponding peptides coupled to CNBr-activated Sepharose. 2 ml of the antiserum were bound to the column at 4°C overnight and washed with TBS. The bound IgG was eluted with 5.0 M $MgCl_2$. The affinity-purified antibodies were then dialyzed against TBS using a Centriprep 30 (Amicon Corp., Danvers, MA).

Preparation of Fusion Proteins and Anti-fusion Protein Antibodies

Glutathione-S-transferase (GST) fusion proteins of α_{1A} (CNA5 and CNA6) were generated by using cDNAs encoding the rbA isoform (Starr et al., 1991) or the human BI (h96) isoform derived from a human small cell carcinoma cell line (Rettig et al., 1995), respectively, as a template and synthetic oligonucleotides with overhanging restriction sites as primers in a PCR. Sequences corresponding to residues 842–981 of rat rbA and 569–712 of the human BI clone were amplified by PCR and cloned into the pGEX-4T expression vector (Pharmacia LKB Biotechnology) to obtain inframe recombinant proteins containing GST. All constructs were verified by DNA sequencing and transformed into a protease-deficient strain BL26 of *Escherichia coli* (Novagen Inc., Madison, WI). Fusion protein expression was performed following the basic protocol of Smith and Johnson

---

1. *Abbreviations used in this paper:* ECL, enhanced chemiluminescence; GST, glutathione-S-transferase; NSF, N-ethylmaleimide–sensitive factor; PAS, protein A–Sepharose; SNAP, soluble NSF attachment protein; SNAP25, synaptosomal-associated protein of 25 kD; SNARE, SNAP receptor; VAMP, vesicle-associated membrane protein.

(1988). In brief, fresh overnight cultures were diluted 1:10 in Luria broth containing ampicillin (100 μg/ml), incubated for 90 min at 37°C with shaking, and induced by addition of 0.5 mM isopropyl-β-D-thiogalactopyranoside. After 2–4 h of growth, bacterial cultures were pelleted by centrifugation at 5,000 g for 10 min at 4°C and resuspended in PBS containing protease inhibitors (4 μg/ml pepstatin, 4 μg/ml aprotinin, 4 μg/ml leupeptin, 0.4 mM PMSF). The bacteria were then lysed by mild sonication, solubilized by adding Triton X-100 to a final concentration of 1%, and incubated for 30 min on ice. The suspension was centrifuged at 15,000 rpm for 15 min, and the supernatant was stored in aliquots at −20°C.

For the production of anti-fusion protein antibodies (anti-CNA5 and anti-CNA6), CNA5 and CNA6 were emulsified in Freund's complete or incomplete adjuvant and injected in New Zealand White rabbits. Antibodies were affinity purified from antisera as described above for the production of anti-peptide antibodies.

Immunoblotting of GST Fusion Proteins and Calcium Channels in Rat and Rabbit Brain

For immunoblotting of CNA5 and CNA6 fusion proteins, 5–10 μg of each fusion protein was treated in SDS sample buffer (200 mM Tris-HCl, pH 6.8, 10 mM dithiothreitol, 4 M urea, 8% SDS, 10% glycerol), separated by SDS-PAGE in 10% acrylamide gels, and transferred onto a nitrocellulose membrane (0.2 μm) in a buffer containing 12.5 mM Tris, pH 8.3, 96 mM glycine, 0.1% SDS, 15% (vol/vol) methanol. Unbound sites on the nitrocellulose were blocked for 2 h at room temperature with TBS containing 10% skim milk powder and incubated with affinity-purified anti-CNA1, anti-CNA3, anti-NBI-1, or anti-NBI-2 antibodies (10–30 μg/ml) in TBS for 2 h at room temperature. After five 5-min washes, blots were incubated for 1 h with HRP–protein A diluted 1:2,000 in TBS. After another six 10-min washes, the blots were developed with the ECL reagent. For peptide block, the corresponding peptides at 2 μM were added to the affinity-purified antibodies and incubated overnight on ice before incubation with samples.

Brain membranes were usually prepared from 15 2-mo-old Sprague-Dawley rats, or from five 3-mo-old New Zealand White rabbits. Brain calcium channels were solubilized with 1.2% digitonin and partially purified by the chromatography on WGA–Sepharose as described previously (Westenbroek et al., 1992, 1995).

For the immunoblotting of rat and rabbit brain membranes, calcium channels in the WGA-column fractions containing 0.1 mg of total protein were concentrated by incubation with 40 μl of heparin-agarose for 4 h on ice (Sakamoto and Campbell, 1991). The resin was washed three times with 10 mM Tris-HCl, pH 7.4, 0.1% digitonin, and once with 10 mM Tris-HCl, pH 7.4. Calcium channels were extracted for 30 min at 50–60°C with 30 μl of SDS sample buffer. After analysis by SDS-PAGE, proteins were transferred onto a nitrocellulose membrane and blocked as described above. Nitrocellulose membranes were incubated with affinity-purified anti-CNA3, anti-NBI-1, or anti-NBI-2 antibodies (10–30 μg/ml), or with affinity-purified anti-CNA5 and anti-CNA6 antibodies (1–3 μg/ml) in TBS for 2 h at room temperature, washed, incubated with HRP–protein A, washed, and treated with ECL reagent as described above. For peptide and fusion protein block, 2 μM of the corresponding peptides or 0.2 μM of the corresponding fusion proteins was added to the affinity-purified antibodies and incubated overnight on ice before incubation with the samples.

Radioactive Ligand Binding Experiments

For [³H]PN-200-110 (isradipine) binding studies, 40 ml of S1 fraction was labeled with 10 μCi of [³H]PN200-110 (85.8 Ci/mmol) at a concentration of 2.9 nM for 1 h on ice. The bound radioligand is stable throughout the subsequent purification steps. Calcium channels were purified from 250 μl of the S3 fraction (~6,000 cpm) containing 300 mM KCl, 150 mM NaCl, 10 mM Tris-HCl, pH 7.4, 1.2% digitonin with 0.2% BSA using 15 μg of affinity-purified anti-CNA3, anti-NBI-1, anti-NBI-2, anti-CNC1, or control rabbit nonimmune IgG. After a 1.5-h incubation on ice, 2.5 mg of PAS, prewashed three times with TBS containing 0.1% digitonin and 0.5% BSA, was added to the samples. The samples were mixed on ice for an additional 2.5 h, pelleted by centrifugation, and washed three times in TBS and 0.1% digitonin. After the final wash, the antibody-bound PAS complexes were transferred to vials, and the amount of immunoprecipitated [³H]PN200-110 receptors was quantified in a scintillation counter. Total receptor-bound [³H]PN200-110 was determined by filter-binding assay. 250 μl of the labeled S3 fraction was precipitated by incubation with 4 ml of ice-cold 10% polyethylene glycol (average mol wt 8,000) in 10 mM

MgCl₂ and 10 mM Tris-HCl, pH 7.4, for 5 min and poured over GF/C filters (Whatman Laboratory Products, Inc., Clifton, NJ). Samples were washed four times in ice-cold polyethylene glycol solution and quantified in a scintillation counter. The correction factor for ligand-receptor loss in the filter-binding assay was 0.7 (Westenbroek et al., 1992).

Determination of [¹²⁵I]ω-conotoxin GVIA binding was done by incubation of 100 μl of S3 fraction containing 0.2% BSA with 0.06 μCi of [¹²⁵I]ω-conotoxin GVIA (2,200 Ci/mmol) at a concentration of 0.27 nM for 30 min on ice. Samples were immunoprecipitated with 15 μg of affinity-purified anti-CNA3, anti-NBI-1, anti-NBI-2, anti-CNB2, or control rabbit IgG, and washed four times with TBS and 0.1% digitonin. The matrix was transferred to the vials for gamma counting. Total [¹²⁵I]ω-conotoxin GVIA binding was determined using 100 μl of the labeled S3 fraction in the filter-binding assay described above for [³H]PN200-110.

[¹²⁵I]ω-conotoxin MVIIC binding was measured by incubation of 400-μl samples containing 140 μl of WGA extract, 10 mM Tris-HCl, pH 7.4, and 0.2% BSA with 0.1 μCi of labeled toxin (1,300 Ci/mmol) at a concentration of 0.15 nM on ice for 30 min. This was added to 15 μg of affinity-purified anti-CNA3, anti-NBI-1, anti-NBI-2, anti-CNC1, or control rabbit IgG, coupled to 2 mg of PAS, and incubated for 4 h on ice in a tilting mixer. Samples were washed quickly three times in 10 mM Tris-HCl, pH 7.4, 75 mM NaCl, 0.1% digitonin, 0.2% BSA. [¹²⁵I]ω-conotoxin MVIIC binding in the pellet was counted in a gamma counter. For competitive displacement studies, the unlabeled ligands ω-conotoxin MVIIC at concentrations ranging from 10⁻¹⁴ to 10⁻⁵ M were added to samples with [¹²⁵I]ω-conotoxin MVIIC, incubated with affinity-purified anti-CNA3 or anti-NBI-2, and the bound [¹²⁵I]ω-conotoxin MVIIC was measured as described above. For peptide block, 20 μM of the corresponding peptides were added to the affinity-purified antibodies and incubated overnight on ice before the incubation with samples containing WGA extract.

Coimmunoprecipitation Studies of α_{1A} with Synaptic Proteins

For the coimmunoprecipitation experiments of α_{1A} with syntaxin and synaptotagmin, a rat brain membrane fraction was prepared according to the procedures described by Lévêque et al. (1994). Briefly, five rat brains were dissected and homogenized in a glass/Teflon homogenizer in buffer A (0.32 M sucrose, 5 mM Tris-HCl, pH 7.4, 1 mM EDTA) on ice, containing protease inhibitors (1 μg/ml pepstatin A, 1 μg/ml leupeptin, 1 μg/ml aprotinin, 0.2 mM PMSF, 0.1 mM benzamidine, and 8 μg/ml calpain inhibitors I and II). After a 5-min centrifugation at 800 g, the supernatant was recovered and spun at 27,000 g for 40 min. Membrane pellets were resuspended and stirred for 15 min on ice in 25 ml of buffer B (3 M urea, 1 mM EDTA, 1 mM dithiothreitol, 5 mM Tris-HCl, pH 7.4) containing protease inhibitors. 100 ml of 0.4 M potassium phosphate, 1 mM EDTA, 1 mM dithiothreitol, 5 mM Tris-HCl, pH 7.4 was added to samples and incubated for 10 min on ice. The membranes were recovered by centrifugation and solubilized in 50 ml of buffer A containing 1.1% CHAPS and 150 mM NaCl. Unsolubilized material was removed by the centrifugation (42,000 rpm, 40 min, Ti 45 rotor), and the supernatant (S3) was stored at −80°C.

0.3 ml of S3 fraction was preabsorbed for 30 min on ice with 150 μl of Sepharose CL-4B and incubated for 1.5 h on ice with 100 μg of control IgG, followed by incubation for 1.5 h on ice with 10 mg of PAS to remove complexes of control IgG with nonspecific binding proteins. After a 1-min centrifugation on a table-top centrifuge, the supernatants were collected and incubated for 3 h on ice with either anti-CNA3 (40 μg), anti-NBI-2 (40 μg), anti-CNB2 (20 μg), anti-SP19 (40 μg), or control antibody (40 μg). The immune complexes were recovered by the incubation on ice for 1.5 h with 4 mg of PAS, washed three times in buffer A containing 1% CHAPS, 150 mM NaCl, and 0.1% BSA, and washed once in 10 mM Tris-HCl, pH 7.4, 1% CHAPS. The pellets were extracted for 30 min at 50–60°C or boiled for 2–3 min with 20 μl of 4% SDS, 12% glycerol, and 0.45 M Tris-HCl, pH 8.45, and analyzed on a Tricine precast gel (Novex Inc., San Diego, CA). Analyzed samples were transferred onto the nitrocellulose membrane, blocked with 10% skim milk in TBST (Tris-buffer saline, pH 7.4, 0.05% Tween-20), and incubated for 1.5 h with a monoclonal anti-syntaxin antibody, mAb10H5 (diluted 1:600,000) (Yoshida et al., 1992). The blots were washed three times in TBST, incubated for 1 h with HRP-conjugated anti–mouse IgG (1:1,000 dilution), washed, and detected with ECL reagent. For the detection of synaptotagmin, we stripped the blots used for detection of syntaxin by the incubation at 50°C for 30 min with Tris-HCl, pH 7.4, containing 2% SDS and 20 mM dithiothreitol. The nitrocellulose sheets were reprobed with mAb1D12, a monoclonal anti-synaptotagmin antibody (diluted 1:1,000) (Lévêque et al., 1992), blocked, in-

cubated with secondary antibodies conjugated with HRP, washed, and visualized as described above.

Immunocytochemistry

2-mo-old Spague-Dawley rats were anesthetized with sodium pentabarbitol, and then intracardially perfused with 4% paraformaldehyde in PB (0.1 M sodium phosphate, pH 7.4) containing 0.34% L-lysine and 0.05% sodium m-periodate (McLean and Nakane, 1974). After removal of the brains from the cranium, they were postfixed for 2 h, and then cryoprotected by sinking in successive solutions of 10, 20, and 30% (wt/vol) sucrose in PB at 4°C over 72 h. Sagittal and coronal sections (40 μm) were cut on a sliding microtome and processed for immunocytochemistry using the avidin–biotin complex method.

Free-floating sections were processed for immunofluorescence by rinsing the tissue in 0.1 M Tris buffer for 5 min, and then rinsing in 0.1 M TBS. To block biotinylated compounds, the tissue was rinsed in a 1% avidin solution in 0.1 M TBS for 30 min, rinsed in 0.1 M TBS for 20 min, put into a 1% solution of biotin in 0.1 M TBS for 30 min, and finally rinsed in 0.1 M TBS for 30 min. The tissue was then incubated in affinity-purified anti-CNA3 (diluted 1:15), anti–NB1-2 (diluted 1:30), or anti–NB1-1 (diluted 1:15) for 1 h at room temperature followed by 36 h at 4°C. All antibodies were diluted in 0.1 M TBS containing 0.1% Triton X-100 and 1% normal goat serum. The sections were rinsed for 1 h in TBS containing 0.1% Triton X-100, incubated in biotinylated goat anti–rabbit IgG (1:300 dilution) for 1 h at 37°C, rinsed in 0.1 M TBS for 15 min, rinsed in 0.1 M Tris buffer for 30 min, mounted onto gelatin-subbed slides, and then coverslipped using Vectashield (Vector Labs, Inc., Burlingame, CA). The immunofluorescent staining was viewed using a confocal microscope (600 MRC; Bio Rad Laboratories, Hercules, CA).

To determine the level of nonspecific staining, some of the control sections were incubated without primary antibody. Other control sections were incubated in primary antibody that had been preincubated for 6–8 h with the corresponding peptide (20 μM) or an unrelated peptide before incubation of the antibody with the tissue. The staining procedure was then carried out as described above. In all of the control sections, the staining patterns reported in this study were abolished in sections treated without primary antibody and when the primary antibody was blocked by the corresponding peptide. The pattern of immunoreactivity remained unaltered when an unrelated peptide was incubated with the primary antibody.

Results

Immunochemical Characterization of Site-directed Anti-peptide Antibodies

Calcium channel α1 subunits are composed of four predominantly hydrophobic homologous domains (I–IV) that are linked by intracellular hydrophilic loops of various length. The homologous domains exhibit a high degree of sequence conservation between subtypes, but the large intracellular loops connecting domains II and III of the neuronal calcium channel α1 subunits are highly variable and characteristic for each class of channels. The BI and rbA isoforms of α_{1A} are different enough in amino acid sequence in the intracellular loop between domains II and III that we were able to select sequences specific for rabbit BI (NBI-1 and NBI-2) and for rat rbA (CNA3) for the production of site-directed anti-peptide antibodies (Fig. 1). The peptide sequence NBI-1 is present in BI, but it is deleted at the equivalent position of rbA. NBI-2 and CNA3 sequences are present at the corresponding positions in BI and rbA, but 11 amino acids are different out of 15 residues. The CNA1 sequence is immediately on the NH$_2$-terminal side of CNA3 in rbA (Sakurai et al., 1995; Westenbroek et al., 1995) and is 60% identical in the equivalent segment of BI (Fig. 1). Thus, antibodies against CNA-1 may be expected to recognize both isoforms. The

corresponding peptides were synthesized, coupled to BSA as a carrier, and used as an antigen for polyclonal antibody production as described in Materials and Methods. In addition, two GST fusion proteins (CNA5 and CNA6) were generated using cDNAs encoding rbA and human BI (hBI), respectively, according to the procedures described in Materials and Methods. CNA5 and CNA6 include the first half of the intracellular loop connecting domains II and III of rbA and BI, respectively, containing the CNA-1, CNA-3, NBI-1, and NBI-2 sequences. In this region, hBI is 90% identical to rabbit BI, while only 33% identical to rbA, and hBI contains identical NBI-1 and NBI-2 sequences as shown in Fig. 1.

The specificity of the polyclonal affinity-purified anti-peptide antibodies (anti–NBI-1, anti–NBI-2, anti-CNA1, and anti-CNA3) for BI and rbA was tested by immunoblotting using CNA5 and CNA6 fusion proteins as antigens (Fig. 2). When CNA5, a GST–rbA fusion protein with a predicted molecular mass of 45 kD, was loaded onto the SDS–polyacrylamide gel, affinity-purified anti-CNA1 and anti-CNA3 antibodies recognized the same immunoreactive band with an apparent molecular mass of 45 kD (Fig. 2 A, lanes 1 and 2). This immunoreactive band was specifically recognized by anti-CNA3, since the preincubation of 2 μM CNA3 peptide completely blocked the interaction of anti-CNA3 with the 45-kD immunoreactive polypeptide, but 2 μM NBI-2 peptide did not affect the immunoreactivity of anti-CNA3 (Fig. 2 A, lanes 3 and 4). In contrast, affinity-purified anti–NBI-1 and anti–NBI-2 antibodies did not reveal any immunoreactive polypeptides in the parallel experiments (Fig. 2 A, lanes 5 and 6). When CNA6, a GST–BI fusion protein with a calculated molecular mass of 45 kD, was analyzed by SDS-PAGE, affinity-purified anti–NBI-1 and anti–NBI-2 antibodies detected the immunoreactive band with an apparent molecular mass of 45 kD and smaller proteins that may be degradation products (Fig. 2 B, lanes 3 and 4). The 45-kD immunoreactive polypeptide was specifically recognized by anti–NBI-2 because preincubation with 2 μM NBI-2 completely blocked the staining of these immunoreactive bands (Fig. 2 B, lane 5). Anti-CNA1 also detected the 45-kD immunoreactive polypeptides, indicating that anti-CNA1 cross-reacts with the corresponding segment of BI (Fig. 2 B, lane 1). In contrast, affinity-purified anti-CNA3 did not recognize any immunoreactive polypeptide (Fig. 2 B, lane 2). These results indicate that affinity-purified anti-CNA3 specifically recognizes rbA, but not BI isoforms of α_{1A}, while affinity-purified anti–NBI-1 and anti–NBI-2 are specific antibodies recognizing BI, but not rbA isoforms of α_{1A}. Anti-CNA1 is not a specific antibody, and therefore it recognizes both BI and rbA in the immunoblot preparation. Based on these immunochemical properties, we used affinity-purified anti–NBI-1, anti–NBI-2, and anti-CNA3 antibodies to identify BI and rbA isoforms of α_{1A} in rat and rabbit brain.

Identification of α_{1A} Polypeptides by Anti–CNA3, Anti–NBI-1, and Anti–NBI-2 in Rat and Rabbit Brain Membranes

To identify α_{1A} polypeptides by anti-peptide antibodies specific for BI and rbA, glycoprotein fractions from rat
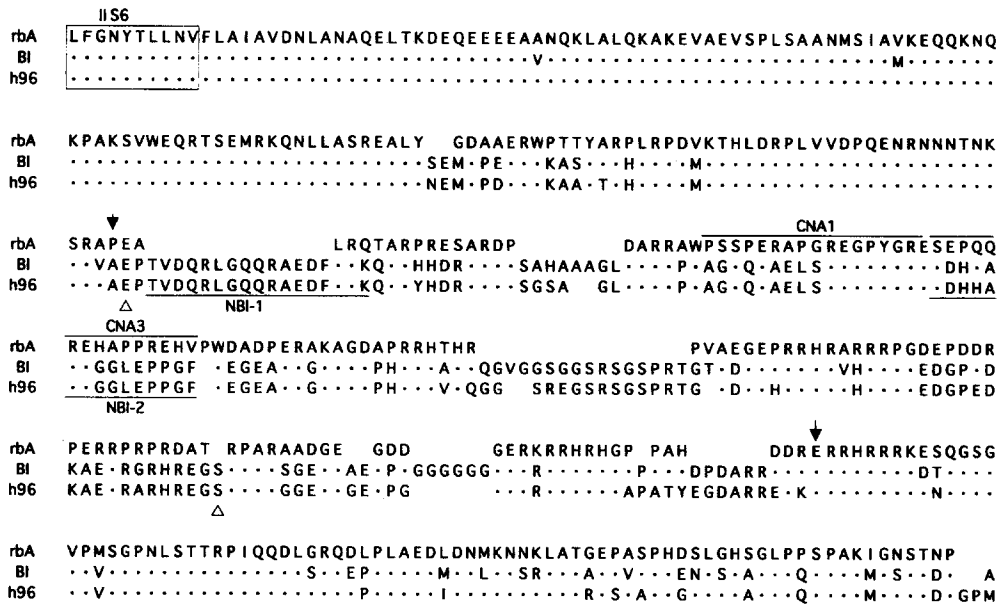
```
        II S6
rbA  |LFGNYTLLNV|FLAIAVDNLANAQELTKDEQEEEEAANQKLALQKAKEVAEVSPLSAANMSIAVKEQQKNQ
BI   |·········|·············································V···················M·······
h96  |·········|·························································
```

```
rbA  KPAKSVWEQRTSEMRKQNLLASREALY   GDAAERWPTTYARPLRPDVKTHLDRPLVVDPQENRNNNTNK
BI   ······························SEM·PE···KAS···H····M·····················
h96  ······························NEM·PD···KAA·T·H····M·····················
```

```
        ▼                                                          CNA1
rbA  SRAPEA            LRQTARPRESARDP          DARRAWPSSPERAPGREGPYGRESEPQQ
BI   ··VAEPTVDQRLGQQRAEDF··KQ··HHDR····SAHAAAGL····P·AG·Q·AELS·········DH·A
h96  ···AEPTVDQRLGQQRAEDF··KQ··YHDR····SGSA  GL····P·AG·Q·AELS·········DHHA
        △       NBI-1
        CNA3
rbA  REHAPPREHVPWDADPERAKAGDAPRRHTHR          PVAEGEPRRHRARRRPGDEPDDR
BI   ··GGLEPPGF ·EGEA··G····PH···A··QGVGGSGGSRSGSPRTGT·D·······VH····EDGP·D
h96  ··GGLEPPGF ·EGEA··G····PH···V·QGG  SREGSRSGSPRTG ·D··H····H····EDGPED
        NBI-2
```

```
rbA  PERRPRPRDAT RPARAADGE  GDD      GERKRRHRHGP PAH      DDRERRHRRRKESQGSG
BI   KAE·RGRHREGS····SGE···AE·P·GGGGGG···R·······P···DPDARR············DT····
h96  KAE·RARHREGS····GGE··GE·PG      ···R······APATYEGDARRE·K··········N····
        △
```

```
rbA  VPMSGPNLSTTRPIQQDLGRQDLPLAEDLDNMKNNKLATGEPASPHDSLGHSGLPPSPAKIGNSTNP
BI   ··V················S··EP·····M·L··SR···A··V···EN·S·A···Q····M·S··D·  A
h96  ··V················P·····I··········R·S·A··G···A···Q····M····D·GPM
```

Figure 1. Design of site-directed anti-peptide antibodies against α_{1A} and GST fusion proteins. Alignment of amino acid sequence (in single letter code) in the first half segment of the intracellular loop between domain II and III of α_{1A} subunits in rat (*top*) (rbA-I; Starr et al., 1991), rabbit (*middle*) (BI; Mori et al., 1991), and human (*bottom*) (h96; Rettig et al., 1996). Amino acid identity is indicated by a dot, and gaps are indicated by spaces. The putative transmembrane segment S6 in domain II is enclosed with solid lines. Peptides (NBI-1, NBI-2, CNA1, and CNA3) chosen to produce site-directed anti-peptide antibodies are illustrated by lines above the protein sequence. Note that amino acid sequences in NBI-1, NBI-2, and CNA1 are completely conserved in rabbit BI and human h96. The arrowheads indicate the first and last residues of the CNA5 (*solid arrowheads*) and CNA6 (*open arrowheads*) fusion proteins that were generated using the rbA (Starr et al., 1991) and h96 cDNAs (Rettig et al., 1996), respectively.

brain were concentrated by affinity chromatography on WGA–Sepharose, and calcium channels were enriched by the adsorption to heparin-agarose and analyzed by immunoblotting (see Materials and Methods). In the rat brain
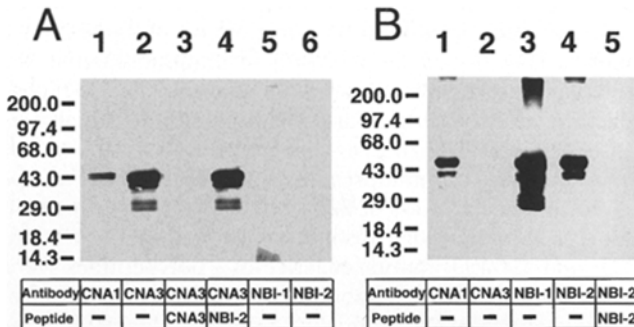

Figure 2. Specific recognition of GST–rbA and GST–BI fusion proteins by anti-peptide antibodies. (*A*) The CNA5 (GST–rbA) fusion protein containing the first half of the cytoplasmic loop connecting domains II and III was analyzed by 10% SDS-PAGE, transferred onto a nitrocellulose sheet, blocked, probed with affinity-purified anti-CNA1 (lane *1*), anti-CNA3 (lanes *2–4*), anti–NBI-1 (lane *5*), and anti–NBI-2 (lane *6*), incubated with HRP–protein A, washed, and visualized with ECL reagent, as described in Materials and Methods. Anti-CNA3 antibodies were preincubated overnight with 2 μM CNA3 peptide (lane *3*) and with NBI-2 peptide at the same concentration (lane *4*). The migration positions of marker proteins are indicated at the left side of the gel together with their molecular masses in kD. (*B*) CNA6 (GST–BI) fusion protein containing the corresponding segment of the intracellular loop between domains II and III was analyzed by SDS-PAGE, blotted, blocked, and probed with affinity-purified anti-CNA1 (lane *1*), anti-CNA3 (lane *2*), anti–NBI-1 (lane *3*), and anti–NBI-2 (lanes *4* and *5*), and detected as described in *A*. Anti–NBI-2 was preincubated with 2 μM NBI-2 peptide (lane *5*).
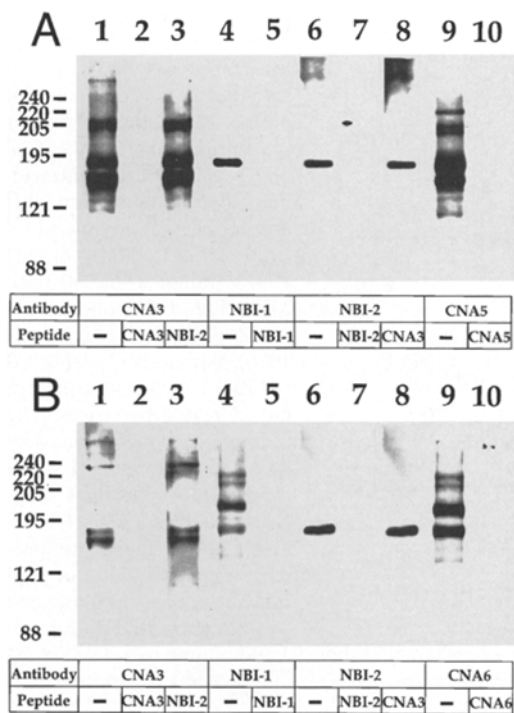
membrane glycoprotein fractions, affinity-purified anti-CNA3 antibodies revealed at least three immunoreactive α_{1A} subunits with apparent molecular masses of 210, 190, and 160 kD (Fig. 3 *A*, lane *1*). These immunoreactive polypeptides were specifically recognized by anti-CNA3, since immunoreactivity against these bands was absorbed by the incubation with 2 μM CNA3 peptide, but not with NBI-2 peptide at the same concentration (Fig. 2 *A*, lanes *2* and *3*). These results agree with previous studies of the biochemical properties of the immunoreactive α_{1A} polypeptides (Sakurai et al., 1995), indicating that the 190-kD form is the major α_{1A} polypeptide, while a doublet with a molecular mass of 210 kD is the minor form. The 190- and 210-kD immunoreactive polypeptides are created by alternative RNA splicing rather than by posttranslational processing of NH_2 or COOH termini (Sakurai et al., 1995). Multiple isoforms of α_{1A} isolated with anti-CNA3 were visualized with affinity-purified anti-CNA5 in parallel experiments. Affinity-purified anti-CNA5 antibody specifically detected five immunoreactive polypeptides with molecular masses of 230, 210, 190, 160, and 120 kD (Fig. 3 *A*, lane *9*). Immunoreactivity for these α_{1A} polypeptides was completely absorbed by the preincubation with 0.2 μM CNA5 fusion protein (Fig. 3 *A*, lane *10*).

Affinity-purified anti–NBI-1 and anti–NBI-2 are specific antibodies to the BI isoform of α_{1A} that has not previously been described in rat brain. Interestingly, affinity-purified anti–NBI-1 specifically recognized an immunoreactive α_{1A} polypeptide with an apparent molecular mass of 190 kD, and labeling was completely blocked by the preincubation of 2 μM NBI-1 peptide in the rat brain membrane glycoprotein fractions (Fig. 3 *A*, lanes *4* and *5*). Affinity-purified anti–NBI-2 also visualized a 190-kD immunoreactive α_{1A} polypeptide (Fig. 3 *A*, lanes *6–8*), and labeling of the 190-kD immunoreactive α_{1A} polypeptide (Fig. 3 *A*, lane

A   1   2   3   4   5   6   7   8   9   10

240 – 220 – 205 – 195 – 121 – 88 –

Antibody	CNA3			NBI-1		NBI-2			CNA5	
Peptide	–	CNA3	NBI-2	–	NBI-1	–	NBI-2	CNA3	–	CNA5

B   1   2   3   4   5   6   7   8   9   10

240 – 220 – 205 – 195 – 121 – 88 –

Antibody	CNA3			NBI-1		NBI-2			CNA6	
Peptide	–	CNA3	NBI-2	–	NBI-1	–	NBI-2	CNA3	–	CNA6

Figure 3. Identification of BI and rbA isoforms of α_{1A} with affinity-purified antibodies in rat and rabbit brain by immunoblotting. (*A*) Membrane glycoprotein fractions were isolated from solubilized rat brain membrane by WGA affinity chromatography, and calcium channels were concentrated by adsorption to heparin agarose, extracted, and analyzed by SDS-PAGE using a 5% acrylamide gel. Proteins were transferred onto a nitrocellulose membrane, blocked, incubated with anti-CNA3 (lanes *1–3*), anti–NBI-1 (lanes *4* and *5*), anti–NBI-2 (lanes *6–8*), or anti-CNA5 (lanes *9* and *10*), incubated with HRP–protein A, washed, and detected with ECL reagent, as described in Materials and Methods. For peptide block, anti-CNA3 antibodies were preincubated overnight on ice with 2 μM CNA3 peptide (lane *2*) or with 2 μM NBI-2 peptide (lane *3*) as a control of the specificity of the peptide block. Anti–NBI-1 was preincubated with 2 μM NBI-1 peptide (lane *5*), and anti–NBI-2 antibodies were preincubated with 2 μM NBI-2 peptide (lane *7*) or with 2 μM CNA3 peptide (lane *8*). Anti-CNA5 was preincubated with 0.2 μM CNA5 fusion protein (lane *10*). The migration positions of α- and β-spectrin, myosin heavy chain, α2-macroglobulin, β-galactosidase, and fructose-6-phosphate kinase are indicated at the left side of the gel together with their molecular masses in kD. (*B*) Rabbit brain membrane glycoprotein fractions were obtained and enriched as described in *A*. Proteins were separated, blotted, blocked, and analyzed with anti-CNA3 (lanes *1–3*), anti–NBI-1 (lanes *4* and *5*), anti–NBI-2 (lanes *6–8*), or anti-CNA6 antibodies (lanes *9* and *10*). Anti-CNA3 antibodies were preincubated with 2 μM CNA3 (lane *2*) or with 2 μM NBI-2 peptide (lane *3*). For peptide block, anti–NBI-1 was preincubated with 2 μM NBI-1 peptide (lane *5*), and anti–NBI-2 antibodies were preincubated with 2 μM NBI-2 peptide (lane *7*) or with 2 μM CNA3 peptide (lane *8*). Anti-CNA6 was preincubated with 0.2 μM CNA6 fusion protein (lane *10*).

6) was completely blocked by preincubation with 2 μM NBI-2 peptide, but not with CNA3 peptide at the same concentration (Fig. 3 *A*, lanes *7* and *8*). These results indicate that anti–NBI-1 and anti–NBI-2 recognize a distinct 190-kD α_{1A} polypeptide from that recognized by anti-

CNA3, and that an isoform of the α_{1A} subunit containing the NBI-1 and/or NBI-2 sequences, referred to here as the BI isoform of α_{1A}, is present in rat brain.

The presence of the BI isoform of α_{1A} in rat brain was also demonstrated in another set of immunoprecipitation experiments, in which exogenous cAMP-dependent protein kinase was used to incorporate ^{32}P into α_{1A} subunits isolated by immunoprecipitation with anti–CNA1, anti–CNA3, anti–NBI-1, and anti–NBI-2 from rat brain membranes (Westenbroek et al., 1993; Sakurai et al., 1995; data not shown). α_{1A} is a substrate for in vitro phosphorylation by several second-messenger–activated protein kinases (Sakurai et al., 1995). Affinity-purified antibodies immunoprecipitated not only radiolabeled α_{1A} polypeptides with a molecular mass of 190 kD, but also those with a molecular mass of 210 kD. These results indicate that the BI isoform of α_{1A} consists of multiple size forms of α_{1A} polypeptides with distinct molecular masses like α_{1A} subunits recognized by anti-CNA3 in Fig. 3 *A*. The 210-kD phosphorylated α_{1A} polypeptides isolated by anti–NBI-1 and –NBI-2 were not detected by immunoblotting, probably because of their low quantity in situ.

If rbA and BI are isoforms of α_{1A} in the rat, it seemed likely that an isoform of α_{1A} with a sequence related to L_{II-III} of rat rbA, referred to as rbA isoform of α_{1A}, is also present in rabbit brain. Therefore, rabbit brain glycoprotein fractions were prepared and analyzed by SDS-PAGE as described above, and rabbit α_{1A} polypeptides were detected by immunoblotting with site-directed anti-peptide antibodies (Fig. 3 *B*). Affinity-purified anti–NBI-1 antibodies visualized multiple immunoreactive α_{1A} polypeptides with apparent molecular masses of 220, 200, and 190 kD (Fig. 3 *B*, lane *4*). Immunoreactivity against all three bands was absorbed by the preincubation of 2 μM NBI-1 peptide (Fig. 3 *B*, lane *5*). Multiple immunoreactive α_{1A} polypeptides in rabbit brain were also specifically recognized by affinity-purified anti-CNA6 antibody, which was raised against GST–BI fusion protein (Fig. 3 *B*, lanes *9* and *10*). The largest immunoreactive polypeptide with an apparent molecular mass of 220 kD was often observed as a doublet band in a high resolution autoradiogram, but the 200- and 190-kD immunoreactive α_{1A} polypeptides were the major size forms in rabbit brain membranes. Affinity-purified anti-NBI-2 specifically recognized the 190-kD immunoreactive polypeptide of α_{1A}, since this band was blocked by the preincubation with 2 μM NBI-2 peptide but was not affected by preincubation with CNA3 peptide at the same concentration (Fig. 3 *B*, lanes *6–8*). Affinity-purified anti-CNA3, an rbA-specific site-directed anti-peptide antibody, detected a major immunoreactive polypeptide with an apparent molecular mass of 190 kD and a minor polypeptide of 230 kD in rabbit brain (Fig. 3 *B*, lane *1*). Preincubation with 2 μM CNA3 peptide, but not with NBI-2 peptide at the same concentration, completely blocked the interaction of anti-CNA3 with the 190- and 230-kD immunoreactive α_{1A} polypeptides (Fig. 3 *B*, lanes *2* and *3*). These results demonstrate that the rbA isoform of α_{1A} is present in the rabbit brain, in addition to the BI isoform, although cDNA encoding rbA was not identified in a rabbit brain cDNA library (Mori et al., 1991). Evidently, rbA and BI are isoforms of α_{1A} present in both rat and rabbit brain.

Immunoprecipitation of High Affinity Receptor Sites for Dihydropyridines, ω-conotoxin GVIA, or ω-conotoxin MVIIC

To determine the pharmacological properties of α_{1A} polypeptides recognized by anti-CNA3, anti-NBI-1, and anti-NBI-2, we labeled rat brain calcium channels with either [^{3}H]PN200-110, [^{125}I]ω-conotoxin GVIA, or [^{125}I]ω-conotoxin MVIIC, and immunoprecipitated labeled rat brain calcium channels with affinity-purified anti-CNA3, anti-NBI-1, or anti-NBI-2 antibodies. [^{3}H]PN200-110 is a dihydropyridine that specifically binds to L-type calcium channels containing α_{1C} and α_{1D} (Dubel et al., 1992). At a concentration of [^{3}H]PN200-110 chosen to saturate all binding sites in a rat brain homogenate, affinity-purified anti-CNC1, an α_{1C}-specific site-directed anti-peptide antibody, immunoprecipitated 40% of total [^{3}H]PN200-110 receptors, while anti-CNA3, anti-NBI-1, and anti-NBI-2 antibodies immunoprecipitated <1%, a value similar to that obtained with control rabbit IgG (Fig. 4 A). The binding of [^{125}I]ω-conotoxin GVIA, a selective conotoxin blocker of N-type calcium channels containing α_{1B}, was tested similarly. Affinity-purified anti-CNB2, an α_{1B}-specific site-directed anti-peptide antibody, immunoprecipitated >80% of the total [^{125}I]ω-conotoxin GVIA binding sites in rat S3 fractions. Under the same conditions, anti-CNA3, anti-NBI-1, anti-NBI-2, and control rabbit IgG immunoprecipitated <4% of the total [^{125}I]ω-conotoxin GVIA receptors (Fig. 4 B). ω-conotoxin MVIIC blocks Q-type calcium channels containing α_{1A} at a low concentration when expressed in Xenopus oocytes (Hillyard et al., 1992; Sather et al., 1993; Stea et al., 1994). A saturating concentration of [^{125}I]ω-conotoxin MVIIC was added to solubilized rat brain membrane fractions enriched by affinity-chromatography on WGA–Sepharose. Affinity-purified anti-CNA3, anti-NBI-1, and anti-NBI-2 antibodies effectively immunoprecipitated [^{125}I]ω-conotoxin MVIIC receptors (Fig. 4 C), while control rabbit IgG immunoprecipitated only small amounts of [^{125}I]ω-conotoxin MVIIC binding sites. Immunoprecipitation of [^{125}I]ω-conotoxin MVIIC receptors with affinity-purified anti-CNA3 was specific, since preincubation of 20 μM CNA3 peptide substantially blocked immunoprecipitation of [^{125}I]ω-conotoxin MVIIC receptors, while CNC1 and NBI-2 peptides at the same concentration did not affect the immunoprecipitation of [^{125}I]ω-conotoxin MVIIC receptors. Immunoprecipitation of [^{125}I]ω-conotoxin MVIIC receptors with affinity-purified anti-NBI-2 was significantly inhibited by the preincubation with 20 μM NBI-2 peptide, but not with 20 μM CNA3 peptide, confirming the specificity of immunoprecipitation. These results indicate that anti-NBI-1/anti-NBI-2 and anti-CNA3 specifically recognize distinct pools of [^{125}I]ω-conotoxin MVIIC receptors in rat brain.

Competitive displacement of specific binding of [^{125}I]ω-conotoxin MVIIC by unlabeled ω-conotoxin MVIIC was tested to determine the affinity of [^{125}I]ω-conotoxin MVIIC receptors recognized by anti-CNA3 and anti-NBI-2. A competitive displacement by unlabeled ω-conotoxin MVIIC was observed between 10 pM and 1 nM with half-maximal inhibition at ~100 pM (Fig. 4 D) in ω-conotoxin MVIIC receptors recognized by affinity-purified anti-CNA3, as previously reported (Sakurai et al., 1995). In contrast,
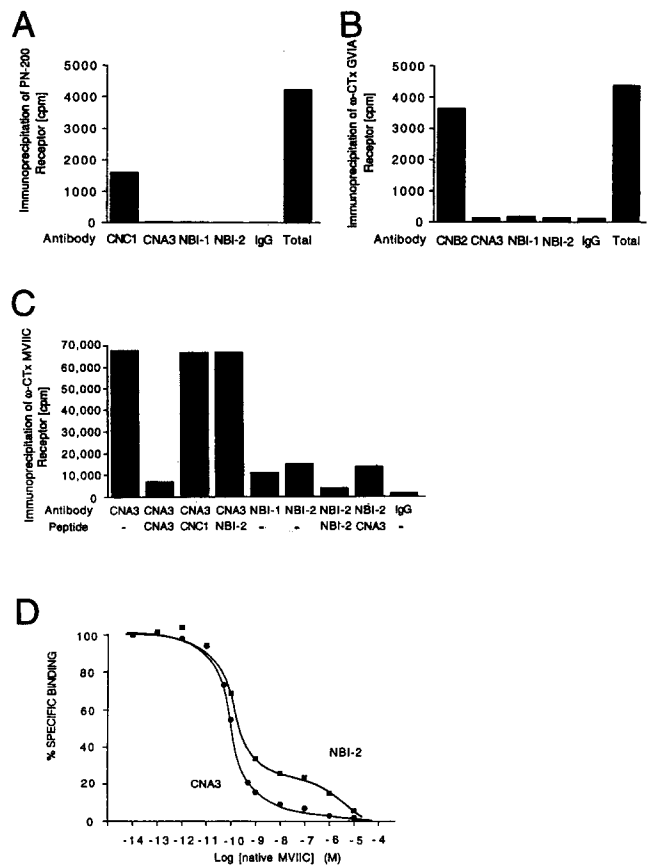

Figure 4. Immunoprecipitation of rat brain calcium channels labeled with [^{3}H]PN200-110, [^{125}I]ω-conotoxin GVIA, or [^{125}I]ω-conotoxin MVIIC. (A) Rat brain membrane fraction was incubated with 2.9 nM [^{3}H]PN200-110, solubilized, immunoprecipitated with anti-CNC1, anti-CNA3, anti-NBI-1, anti-NBI-2, or rabbit nonimmune control IgG, and bound [^{3}H]PN200-110 was counted (see Materials and Methods). Anti-CNC1 was raised against a highly variable site of the class C L-type calcium channel α1 subunit and is specific for α_{1C} (Hell et al., 1993). Total [^{3}H]PN200-110 receptor sites were estimated by filter binding assay. (B) Rat brain membrane fractions were incubated with [^{125}I]ω-conotoxin GVIA (0.27 nM) and immunoprecipitated with anti-CNB2, anti-CNA3, anti-NBI-1, anti-NBI-2, or control IgG. Anti-CNB2 is specific for class B N-type calcium channel α1 subunit (Westenbroek et al., 1992). (C) Calcium channels were purified from rat brain membranes by chromatography on WGA–Sepharose, incubated with [^{125}I]ω-conotoxin MVIIC (0.15 nM), and immunoprecipitated with anti-CNA3, anti-NBI-1, anti-NBI-2, anti-CNC1, or control IgG. The specificity of immunoprecipitation of [^{125}I]ω-conotoxin MVIIC receptors with anti-CNA3 was tested by block with the indicated peptides. Anti-CNA3 was preincubated with 20 μM CNA3 peptide, 20 μM CNC1 peptide, or 20 μM NBI-2 peptide, and immunoprecipitation was carried out as described in Materials and Methods. Anti-NBI-2 antibodies were preincubated with 20 μM NBI-2 or with 20 μM CNA3 peptide for peptide block experiments. (D) The indicated concentrations of ω-conotoxin MVIIC were added to WGA-purified samples with [^{125}I]ω-conotoxin MVIIC (0.15 nM) and immunoprecipitated with affinity-purified anti-CNA3 (filled circles) or with anti-NBI-2 antibodies (filled squares). Bound [^{125}I]ω-conotoxin MVIIC was determined, and the values were normalized to the specific binding observed in the absence of unlabeled toxin (100%). A mean value was calculated from data pooled from three independent experiments (n = 5–7).

[^{125}I]ω-conotoxin MVIIC receptors immunoprecipitated with affinity-purified anti–NBI-2 were competitively displaced by unlabeled ω-conotoxin MVIIC in a biphasic manner (Fig. 4 D), suggesting the possibility of more than one binding site for ω-conotoxin MVIIC. The IC$_{50}$ of the high affinity site for ω-conotoxin MVIIC was ∼100 pM, which is a similar value obtained in the ω-conotoxin MVIIC receptors immunoprecipitated with anti-CNA3, and the IC$_{50}$ of the low affinity site for ω-conotoxin MVIIC was ∼1 μM. The low affinity receptor sites for ω-conotoxin MVIIC recognized by anti–NBI-2 were not ω-conotoxin GVIA binding sites, because anti–NBI-2 immunoprecipitated <4% of total ω-conotoxin GVIA receptors (Fig. 4 B). Evidently, the pharmacological properties of a fraction of [^{125}I]ω-conotoxin MVIIC receptors immunoprecipitated with anti–NBI-2 are distinct from those recognized by anti-CNA3 in rat brain.

Coimmunoprecipitation of α$_{1A}$ Subunits with Syntaxin and Synaptotagmin

On the basis of immunocytochemical localization and electrophysiological findings, class B N-type calcium channels and class A P/Q-type calcium channels are implicated in fast synaptic neurotransmission (Llinas et al., 1992; Horne et al., 1991; Takahashi and Momiyama, 1993; Luebke et al., 1993; Wheeler et al., 1994; Westenbroek et al., 1992, 1993, 1995). Coimmunoprecipitation and calcium channel purification experiments have indicated that N-type channels are associated with synaptic proteins, such as syntaxin and synaptotagmin (Bennett et al., 1992; Lévèque et al., 1994; Yoshida et al., 1992) through interaction with the intracellular loop between domains II and III (Sheng et al., 1994, 1996), and that the N-type channel is a component of a prefusion docking complex for synaptic vesicles (for review see Jahn and Südhof, 1994). Therefore, it is likely that class A calcium channels are also associated with syntaxin and synaptotagmin. To determine if the α$_{1A}$ subunits recognized by anti-CNA3 and anti–NBI-2 are associated with synaptic proteins, we examined the association of α$_{1A}$ subunits with syntaxin and synaptotagmin by coimmunoprecipitation experiments (Fig. 5). Rat brain homogenates were washed in Tris-HCl buffer, pH 7.4, containing 3 M urea, 1 mM EDTA, and 1 mM dithiothreitol, and solubilized with 1.1% CHAPS as described in Materials and Methods. Calcium channel α1 subunits were isolated by immunoprecipitation with either affinity-purified anti-CNA3, anti–NBI-2, or anti-CNB2, an α$_{1B}$-specific site-directed anti-peptide antibody, and samples were treated with SDS sample buffer at 50–55°C for 30 min and analyzed by SDS-PAGE. Coimmunoprecipitated proteins of interest were first probed with an mAb (mAb10H5) that recognizes syntaxin 1A and 1B (Yoshida et al., 1992) (Fig. 5 A). Syntaxin 1A and 1B are 35-kD synaptic proteins anchored by their COOH termini in the presynaptic plasma membrane (Bennett et al., 1992; Inoue et al., 1992; Yoshida et al., 1992). In the samples immunoprecipitated with affinity-purified anti-CNB2, anti-CNA3, and anti–NBI-2, mAb10H5 detected two predominant immunoreactive bands with apparent molecular masses of 90 and 35 kD, and some other bands >90 kD showed faint signals (Fig. 5 A, lanes 1 and 3; data not shown for NBI-2 samples). However, specificity of immunoprecipitation of syntaxin was not complete.

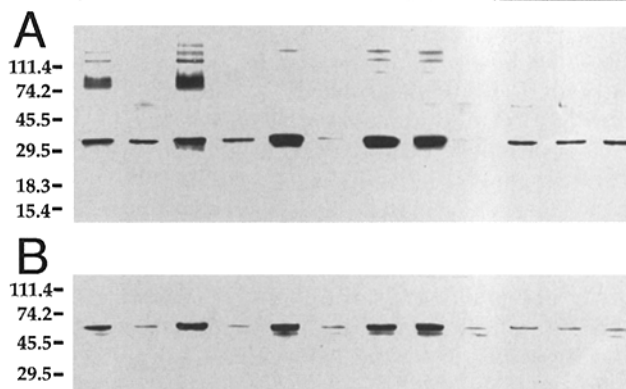| Ab	CNB2		CNA3					NBI-2		SP-19		IgG
Pep	–	B2	–	A3	–	A3	C1	–	BI-2	–	SP	–
Boil	–	–	–	–	+	+	+	+	+	–	–	–
Lane	1	2	3	4	5	6	7	8	9	10	11	12

Figure 5. Coimmunoprecipitation of syntaxin and synaptotagmin with α$_{1A}$ by anti-CNA3 and anti–NBI-2 in rat. Rat brain membranes were washed and solubilized with 1.1% CHAPS as described in Materials and Methods. Calcium channel α1 subunits were isolated by immunoprecipitation with 40 μg of anti-CNB2 (lanes 1 and 2), anti-CNA3 (lanes 3–7), anti–NBI-2 (lanes 8 and 9), anti-SP19 (lanes 10 and 11), or control IgG (lane 12). Anti-SP-19 is a site-directed anti-peptide antibody against type II brain sodium channel (West et al., 1991). Immunoprecipitation was performed after preincubation with 20 μM CNB2 (lane 2), CNA3 (lanes 4 and 7), CNC1 (lane 7), NBI-2 (lane 9), and SP-19 (lane 11) peptides. Samples were incubated with SDS sample buffer at 50–55°C for 30 min (lanes 1–4, 10, and 11) or boiled for 2–3 min (lanes 5–9 and 12), and then analyzed by SDS-PAGE on a precast tricine gel, blotted, and probed with mAb10H5, an mAb against syntaxin (Yoshida et al., 1992) (A), and with mAb1D12, an mAb against synaptotagmin (Lévèque et al., 1992) (B). The migration positions of marker proteins are indicated at the left side of the gel together with their molecular masses in kD.

The 35-kD immunoreactive band was substantially reduced but still weakly visualized in the immunoprecipitated samples after preincubation with 20 μM CNB2 and CNA3 peptide (Fig. 5 A, lanes 2 and 4), with anti-SP19, a site-directed anti-peptide antibody against brain sodium channel type IIA (Gordon et al., 1988; Fig. 5 A, lanes 10 and 11), and with nonimmune IgG (Fig. 5 A, lane 12). In contrast, the 90-kD and larger immunoreactive bands were specifically coimmunoprecipitated with anti-CNB2, anti-CNA3, and anti–NBI-2, since these immunoreactive bands were completely blocked by preincubation of 20 μM corresponding peptides (Fig. 5 A, lanes 2 and 4; data not shown for NBI-2 samples), and the 90-kD band was not visualized in the samples immunoprecipitated with anti-SP19 and with control rabbit IgG (Fig. 5 A, lane 12).

The synaptic proteins syntaxin, synaptosomal-associated protein of 25 kD (SNAP25), and synaptobrevin/vesicle-associated membrane protein (VAMP) form an SDS-resistant complex that is stable to exposure at temperature up to 60°C for 5 min and may function in synaptic vesicle docking and fusion (Hayashi et al., 1994; Chapmann et al., 1994). To test if the 90-kD syntaxin complexes detected by mAb10H5 are stable, SDS-resistant complexes, we incu-

bated the immunoprecipitated samples for 2–3 min in boiling water instead of at 50°C and probed with mAb10H5. After boiling, mAb10H5 recognized a single immunoreactive band with a molecular mass of 35 kD in the immunoprecipitated samples with anti-CNB2, anti-CNA3, and anti–NBI-2 (Fig. 5 A, lanes 5–9; data not shown for CNB2 samples). The signal of the 35-kD immunoreactive band was more intense than in samples that were immunoprecipitated with anti-CNA3 and incubated at 50°C (Fig. 5 A, lanes 3 and 5). In boiled samples, the 35-kD immunoreactive bands were specifically coimmunoprecipitated with anti-CNA3, since preincubation with 20 μM CNA3 peptide completely blocked immunoprecipitation of the 35-kD band, while CNC1 peptide at the same concentration did not affect coimmunoprecipitation with syntaxin (Fig. 5 A, lanes 5–7). The specificity of the 35-kD immunoreactive bands in the samples immunoprecipitated with anti–NBI-2 and anti-CNB2 was tested by peptide block similarly (Fig. 5 A, lane 9; data not shown for CNB2 samples). Thus, the 90-kD complex detected in samples incubated at 50°C was an SDS-resistant complex containing syntaxin and was specifically coimmunoprecipitated with the α_{1B} and α_{1A} subunits recognized by anti-CNB2, anti-CNA3, and anti–NBI-2 in rat brain.

We also tested the association of class A calcium channels with synaptotagmin, a 65-kD synaptic vesicle protein containing a transmembrane domain in NH_2-terminal region and calcium binding domains (C2 repeats) in COOH terminus (Matthew et al., 1981; Jahn and Südhof, 1994). We stripped the membrane used for the detection of syntaxin and probed with mAb1D12 an mAb against synaptotagmin (Lévèque et al., 1992) (Fig. 5 B). In the samples immunoprecipitated with affinity-purified anti-CNB2, mAb1D12 detected a single immunoreactive band with an apparent molecular mass of 65 kD, which was blocked by the preincubation with 20 μM CNB2 peptide (Fig. 5 B, lanes 1 and 2). These results support previous findings that synaptotagmin is associated with class B N-type calcium channels (Lévèque et al., 1992, 1994) and that synaptotagmin is not included in the SDS-resistant complex (Hayashi et al., 1994). Synaptotagmin was specifically coimmunoprecipitated with affinity-purified anti-CNA3 and anti–NBI-2 antibodies, since mAb1D12 detected much less intense bands in the immunoprecipitated samples after preincubation of the antibodies with the corresponding peptides at 20 μM (Fig. 5 B, lanes 1–9), or in samples immunoprecipitated with anti-SP19 or control rabbit IgG (Fig. 5 B, lanes 10–12). These results indicate that α_{1A} subunits recognized by anti-CNA3 and anti–NBI-2 are associated with synaptotagmin as well as with syntaxin, and therefore are implicated in synaptic vesicle docking and fusion at presynaptic terminals in the rat brain.

Differential Subcellular Localization of the rbA and BI Isoforms of α_{1A} in the Cerebellum

α_{1A} subunits recognized by anti-CNA3 or anti–NBI-2 antibodies are differentially distributed in cell bodies, in dendrites, in punctate structures located in regions rich in synapses, and in punctate structures associated with cell bodies and dendrites. Based on previous studies showing that similar punctate clusters of α_{1A} are presynaptic and

are colocalized with presynaptic membrane protein syntaxin (Westenbroek et al., 1993, 1995), the punctate labeling pattern likely represents staining of class A calcium channels in presynaptic nerve terminals.

The most prominent staining with anti–NB1-2 and anti-CNA3 was observed in the cerebellum. Both antibodies stained Ca^{2+} channels in the granular, Purkinje cell, and molecular layers of the cerebellum (Fig. 6). Anti–NB1-2 exhibited relatively dense staining along the length of Purkinje cell dendrites with moderate staining of the Purkinje cell body (Fig. 6 A). Punctate staining of nerve terminals was observed in both the granular and molecular layers (Fig. 6 A). This pattern of staining was similar to that observed using anti-CNA1 antibodies previously (Westenbroek et al., 1995). In contrast, the most dense staining with the anti-CNA3 antibody was observed in the soma of Purkinje cells, with moderate levels of staining in the dendrites of Purkinje neurons and in nerve terminals throughout the granular and molecular layers but comparatively little staining of dendrites (Fig. 6 D). No staining was observed when the primary antibody was eliminated from the procedure (not shown), and staining by each of the antibodies was blocked when they were preincubated with their corresponding peptides (Figs. 6, B and E). In contrast, the pattern of staining was unaltered when anti–NB1-2 was preincubated with the CNA3 peptide (Fig. 6 C) or when anti-CNA3 was preincubated with the NB1-2 peptide (Fig. 6 F). These results indicate that the anti-CNA3 antibody, which is specific for the rbA isoform, and the anti–NBI-2 antibody, which is specific for the rabbit BI isoform, do not cross-react and specifically recognize α_{1A} subunits with different subcellular distributions.

A more detailed analysis of the staining in the molecular layer of the cerebellum revealed low intensity staining with anti–NBI-2 along the surface of the Purkinje cell dendrites located in the deeper half of the molecular layer adjacent to the Purkinje cell body layer with superimposed punctate accumulations of stain representing nerve terminals (Fig. 7 A). Staining of dendritic surfaces with the NBI-2 antibody is less apparent in the distal portions of the Purkinje cell dendritic field where only a random pattern of punctate nerve terminals was observed (Fig. 7 B). Dendritic staining was less prevalent with anti-CNA3 (Fig. 7 C), indicating preferential localization of the BI isoform relative to the rbA isoform in the dendrites of Purkinje neurons. However, there is relatively intense punctate staining of nerve terminals, which often appears to follow the contour of the faintly labeled dendritric branches located both proximal (Fig. 7 C) and distal (Fig. 7 D) to the Purkinje cell soma. At higher magnification, the pattern of immunoreactivity in the granule cell layer is very similar for both antibodies (Fig. 8, A and B). We observed staining of punctate structures around the cell bodies of neurons located throughout the granular layer as well as immunoreactivity in punctate structures in the surrounding glomeruli where synaptic complexes are formed among granule cells, Golgi cells, and incoming mossy fibers.

Differential Localization of rbA and BI Isoforms of α_{1A} in the Hippocampus

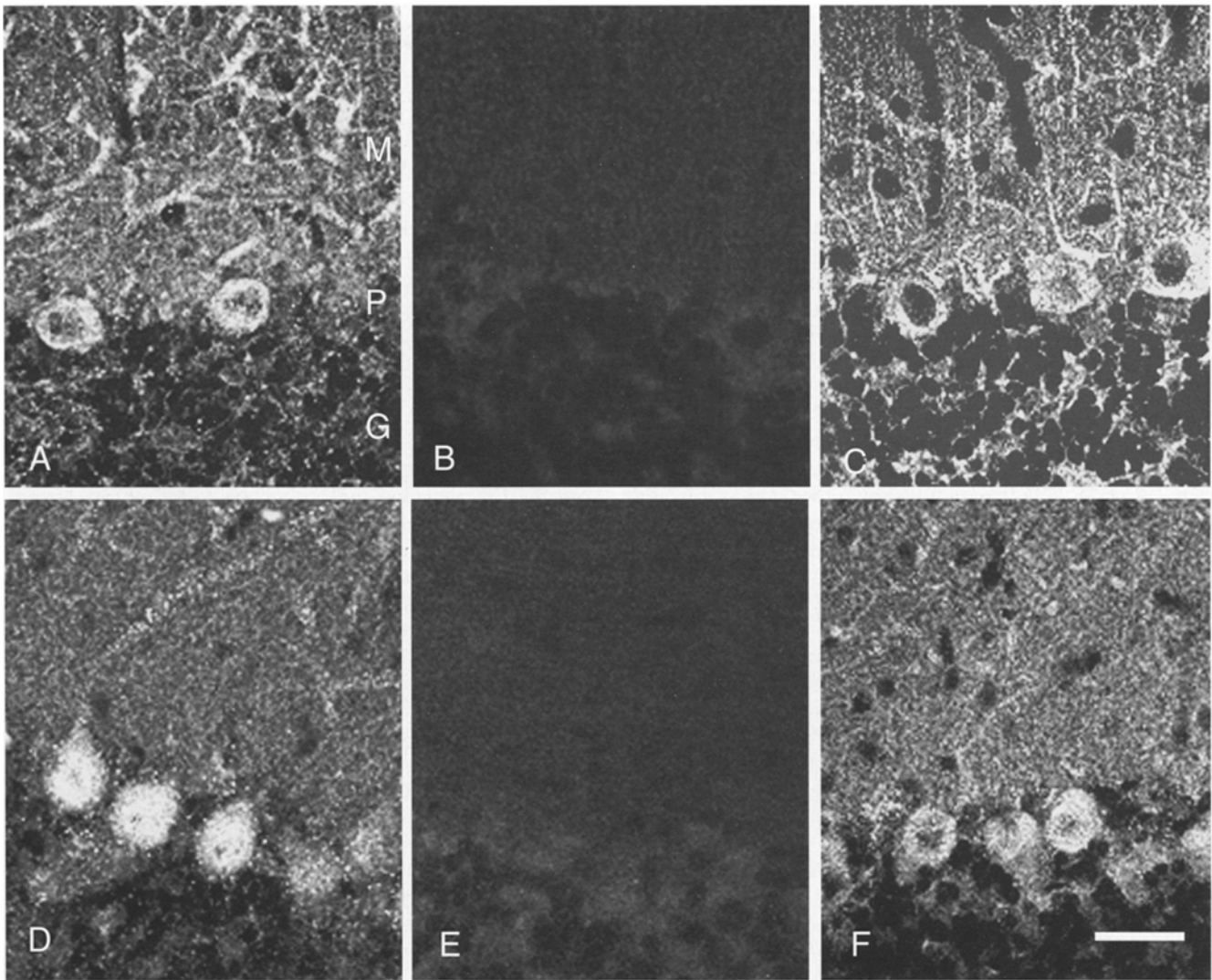In the CA1 region of the hippocampus, both antibodies

Figure 6. Distribution of α_{1A} isoforms in the cerebellum. Sagittal sections of adult rat brain were stained with anti-CNA3 or anti–NB1-2 using the immunofluorescence technique described in the Materials and Methods. (*A*) Low magnification of anti–NB1-2 staining in the cell body and dendrites of Purkinje cells. (*B*) Control section stained with anti–NB1-2 antibody that was preincubated with the NB1-2 peptide to demonstrate that specific staining is blocked by the peptide. (*C*) Control section incubated with anti–NB1-2 antibodies that were preincubated with the CNA3 peptide to illustrate that the staining pattern is unaltered. (*D*) Tissue section stained with anti-CNA3 antibodies illustrating strong immunoreactivity in the cell body of Purkinje neurons and weak immunoreactivity in the dendrites. (*E*) Control section incubated with anti-CNA3 antibody preincubated with the CNA3 peptide, demonstrating the absence of staining in the presence of the peptide. (*F*) Control section incubated with anti-CNA3, which was preincubated with the NB1-2 peptide to illustrate that the pattern of immunoreactivity remained unaltered. Bar, 50 μm.

stained punctate synaptic structures. However, anti–NBI-2 staining was prominent in dendrites (Fig. 9 *A*), whereas staining by anti-CNA3 was more prominent in cell bodies (Fig. 9 *D*). Analysis at higher magnification reveals that the staining for α_{1A} subunits recognized by anti–NBI-2 extends along the entire length of the apical dendrites (Fig. 9, *B* and *C*). There is smooth staining along the dendritic surface with punctate labeling of nerve terminals superimposed upon the dendrites as well as punctate labeling of nerve terminals in the surrounding neuropil (Fig. 9, *B* and *C*). In contrast, anti-CNA3 antibodies labeled mainly the cell bodies of pyramidal neurons and interneurons in the CA1 region of the hippocampus (Fig. 9 *D*). At higher magnification, it appears that there is also punctate staining of

nerve terminals in both the superficial (Fig. 9 *E*) and deep regions (Fig. 9 *F*) of the stratum radiatum.

In the CA3 region of the hippocampus, anti–NBI-2 stained predominantly the pyramidal neuron cell bodies and dendrites (Fig. 10 *A*). There was relatively dense, smooth staining of the proximal dendritic surface as well as some nerve terminals, which appeared as small punctate structures (Fig. 10 *B*). This coincides with the region of termination of the axons of the dentate granule neurons (the mossy fibers), making it difficult to determine if the mossy fiber terminals themselves are also labeled at a low level. Along the distal portions of CA3 dendrites, anti–NBI-2 labels both the dendritic surface and nerve terminals (Fig. 10 *C*).

In contrast with the pattern of staining with anti-NBI-2,
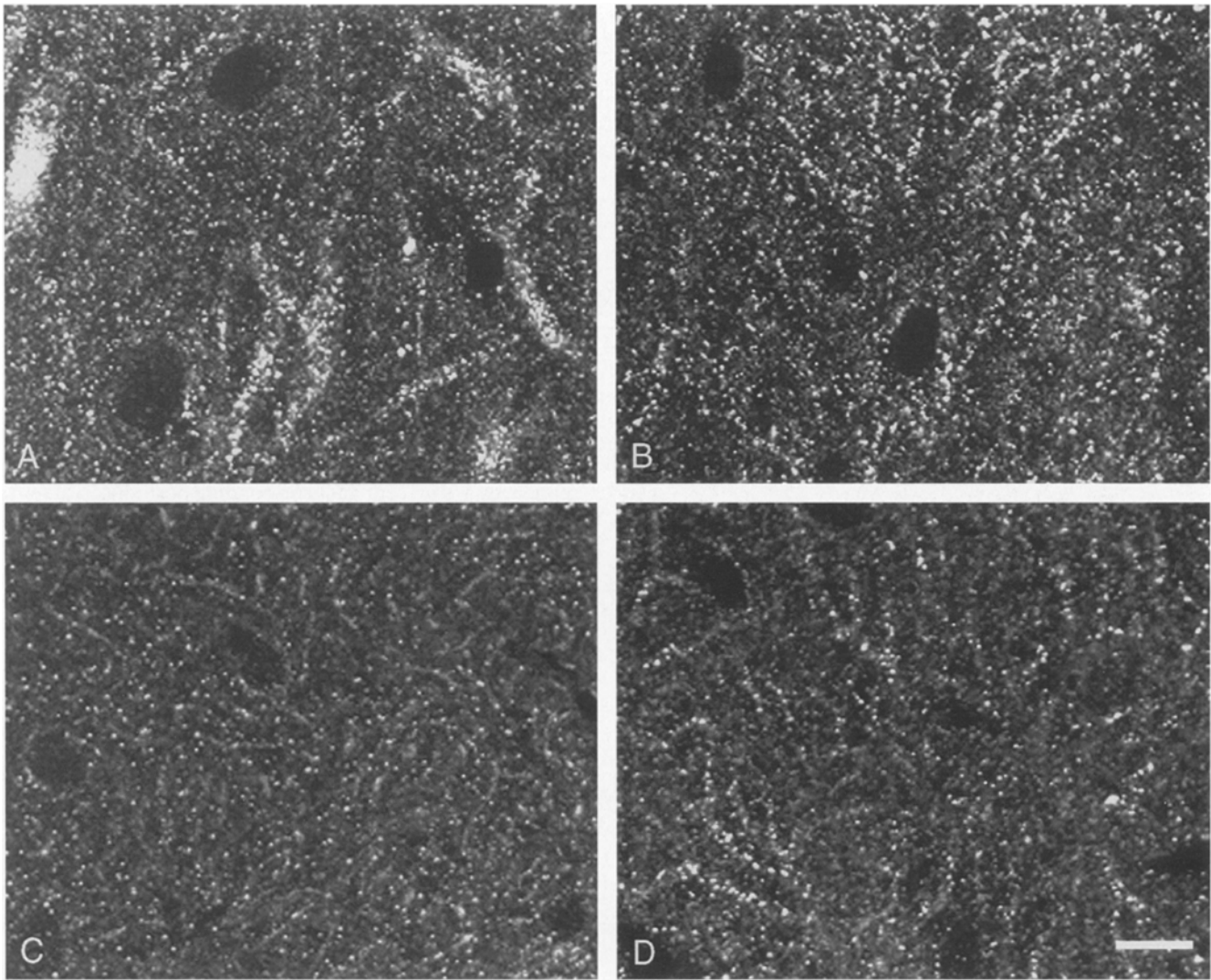
Figure 7. Localization of rbA and BI in the molecular layer of the cerebellum. Sagittal sections of adult rat brain were stained with anti-CNA3 or anti–NB1-2 using the immunofluorescence technique described in Materials and Methods. (*A*) Higher magnification view of staining with the anti–NB1-2 antibody immunoreactivity in the middle portion of the molecular layer, illustrating low intensity staining along dendrites and staining of punctate structures superimposed upon the dendritic staining and in the surrounding neuropil. (*B*) Section from the superficial portion of the molecular layer, demonstrating anti–NB1-2 staining in punctate structures. (*C*) Staining of anti-CNA3 in punctate structures located in the middle portion of the molecular layer. (*D*) Localization of anti-CNA3 in the superficial layer of the molecular layer in punctate structures. Bar, 25 μm.

anti-CNA3 densely stained the large nerve terminals of the mossy fibers along the proximal dendrites of CA3 pyramidal neurons, but stained the dendrites much less intensely (Fig. 10, *D* and *E*). Labeling of large nerve terminals was observed scattered thoughout the cell body layer as well as along the proximal portion of the dendrites. Relatively low levels of labeling were observed on the cell bodies of CA3 neurons with the anti-CNA3 antibody (Fig. 10 *D*). Dense immunoreactivity was observed in punctate structures representing nerve terminals throughout the entire layer in which the apical dendrites of CA3 neurons reside (Fig. 10 *F*). These results indicate preferential localization of the rbA isoform in the nerve terminals of the mossy fibers making synapses on the proximal dendrites of CA3 neurons, and in the nerve terminals of other fibers making synapses on the distal dendrites of CA3 neurons.

Localization of the rbA and BI Isoforms of α_{1A} in Dorsal Cerebral Cortex

Dense labeling of dendrites with anti–NBI-2 was observed throughout the dorsal cortex (Fig. 11, *A* and *B*). Dendritic labeling was common to all types of neurons and was associated with both large and small diameter dendrites (Fig. 11, *A* and *B*). Dense, smooth staining along the dendritic surface as well as punctate labeling of nerve terminals superimposed on the smooth dendritic staining was observed. In addition, there was labeling of the cell bodies of some cortical neurons. The most dense cell body labeling was associated with the large pyramidal neurons of layers 4/5. The cell bodies of neurons in the other layers of the dorsal cortex were sometimes lightly labeled.

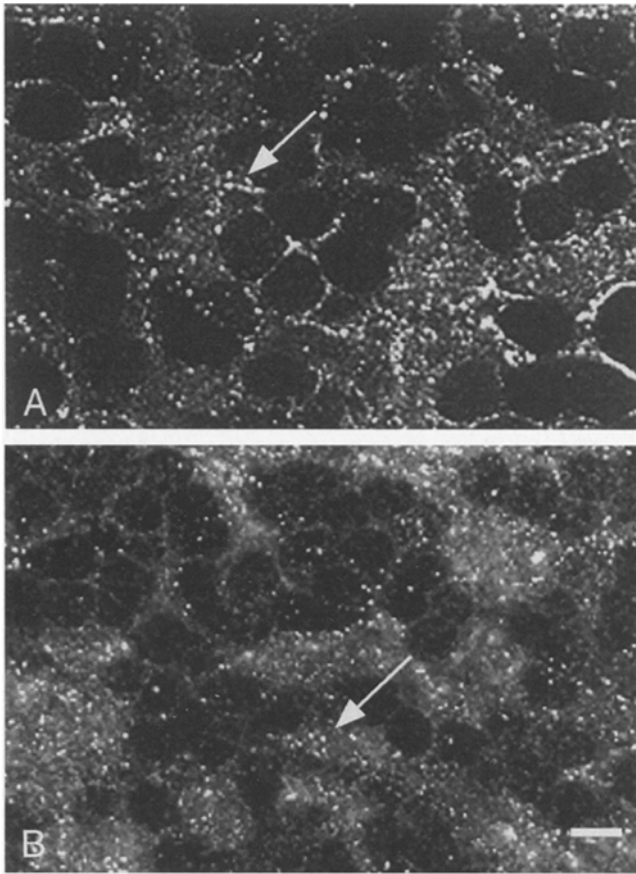The cell bodies of neurons throughout all layers of the

Figure 8. Distribution of α_{1A} isoforms in the granule cell layer of the cerebellum. Sagittal sections of adult rat brain were incubated with anti-CNA3 or anti–NB1-2 as described in Materials and Methods. Tissue sections of the granule cell layer of the cerebellum, demonstrating the similar pattern of punctate staining around cell bodies and in regions of synaptic complexes (*arrows*) using either anti–NBI-2 (*A*) or anti-CNA3 (*B*) antibodies. Bar, 10 μm.

dorsal cortex were immunoreactive for anti-CNA3 (Fig. 11, *C* and *D*). At higher magnification, it is apparent that this antibody lightly labels the surface of the cell body and punctate structures in the surrounding neuropil (Fig. 11 *D*). Cytoplasmic staining around the nucleus by anti-CNA3 was prominent in neurons located in the dorsal cortex (Fig. 11 *D*). This pattern of staining was also present in the hippocampus and other regions of the brain and may represent staining of the Golgi complex where membrane proteins are processed before being inserted into the plasma membrane. In contrast with anti–NBI-2, anti-CNA3 did not stain the dendrites of cortical neurons detectably, indicating a preferential localization of the BI isoform of α_{1A} in cortical dendrites.

Discussion

BI and rbA Isoforms of α_{1A} Are Both Present in Rat and Rabbit Brain

Previous cDNA cloning studies defined the primary struc-

tures of the rbA and BI isoforms of α_{1A} in rat and rabbit brain, respectively (Starr et al., 1991; Mori, 1991). It has been assumed that these two isoforms represent the same gene product in two distinct species. We were led to examine this issue more closely by comparison of the amino acid sequences of each segment of these two isoforms. This comparison reveals that the intracellular loop between domains II and III (L_{II-III}) is strikingly divergent (only 78% identical) compared with the remainder of the protein (>98% identical in all other regions except the COOH-terminal region). In these experiments, we have used anti-peptide antibodies to provide direct evidence that both the BI isoform of α_{1A} containing the NBI-1 and/ or NBI-2 sequences and the rbA isoform of α_{1A} containing the CNA3 sequence are present in both rat and rabbit brain by immunoblotting, immunoprecipitation, and immunocytochemistry. Sequence NBI-1 has been identified only in the rabbit BI isoform, while the NBI-2 and CNA3 sequences are present at corresponding positions in cDNAs encoding BI and rbA, respectively (Fig. 1). Our results and the comparison of sequence identity in different regions of the BI and rbA sequences suggest that alternative mRNA splicing may give rise to the difference in amino acid sequence in L_{II-III} between these two distinct cDNAs (BI and rbA) encoding class A calcium channel $\alpha1$ subunits. Consistent with alternative splicing in this region, an insertion/deletion of 349 residues (772–1,120) in the intracellular loop between domains II and III was identified in the initial cloning of the BI isoform (Mori et al., 1991). Anti-CNA3 and anti–NBI-2 would not be able to recognize isoforms of α_{1A} with this segment deleted. Therefore, there may be additional isoforms of α_{1A} that are not detected in our experiments. To identify all of the alternative splicing sites in the intracellular loop between domains II and III of α_{1A}, an analysis of intron/exon organization of the α_{1A} gene is required.

The amino acid sequence similarity between the BI and rbA isoforms is also relatively low in the COOH-terminal region (85%). For rabbit BI, two different length mRNAs have been isolated, differing in the COOH-terminal region (BI-1 and BI-2) (Mori et al., 1991). An additional substitution was identified in the COOH terminus of BI (sequence a and sequence b containing 28 amino acids, residues 1,857–1,884), resulting in two more potential combinations that may be represented in mRNAs. In rat rbA, four distinct transcripts were detected by Northern blot analysis (Starr et al., 1991) and two isoforms (rbA-I and rbA-II) that are apparently products of alternative RNA splicing (Soong et al., 1994) were identified. Sequence b is also present in the COOH terminus of rbA, at the equivalent position as in BI. Thus, it is likely that there is also extensive alternative splicing of the COOH terminus of α_{1A} and that multiple combinations of alternative exons in L_{II-III} and the COOH terminus may result in further diversity of the isoforms of α_{1A}.

Antibodies against α_{1A} recognize a diverse array of polypeptides in rat and rabbit brain ranging in apparent molecular mass from 230 kD to 160 kD (Sakurai et al., 1995; this paper). A 190-kD polypeptide is the most prevalent size form in all cases, and there are larger size forms present in lesser amounts that are recognized by both anti-CNA3 and anti–NBI-2 in both rat and rabbit brain. Previ-
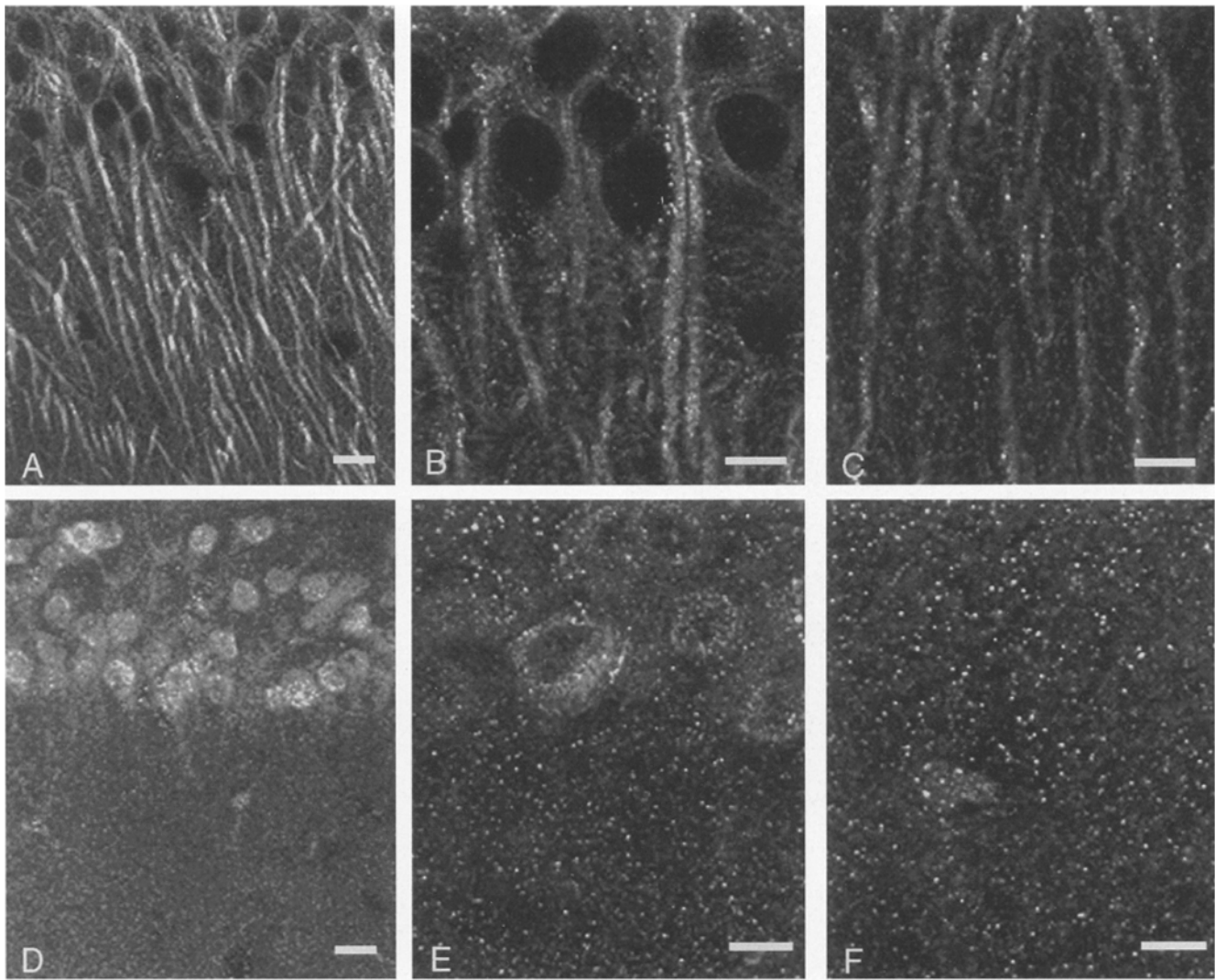
Figure 9. Localization of α_{1A} isoforms in the CA1 region of the hippocampus. Sagittal sections of adult rat brain reacted with anti-CNA3 or anti–NB1-2 antibodies using the immunofluorescence technique described in Materials and Methods. (*A*) Tissue section stained with anti–NBI-2, demonstrating dense staining of dendritic surfaces of CA1 pyramidal neurons. (*B*) Higher magnification of anti–NBI-2 staining along the proximal portions of CA1 pyramidal neuron dendrites. Superimposed upon the smooth staining of dendrites is the staining of punctate structures. (*C*) Higher magnification of anti–NBI-2 staining along the distal portions of the apical dendrites, illustrating both smooth staining of dendritic surfaces with staining of punctate structures superimposed upon them. (*D*) Tissue section stained with anti-CNA3, illustrating localization of α_{1A} in the cell bodies of CA1 pyramidal neurons. (*E*) A higher magnification picture of anti-CNA3 staining in the cell soma and in punctate structures in the regions of the proximal portions of the apical dendrites. (*F*) Anti-CNA3 staining in the stratum radiatum, illustrating the localization of α_{1A} in punctate structures in the region where the distal dendrites of CA1 pyramidal neurons reside. Bars: (*A*, *D*, and *G*) 50 μm; (*B*, *C*, *E*, *F*, *H*, and *I*) 25 μm.

ous studies show that the 220- and 190-kD size forms have the NH_2 and COOH termini encoded by the full-length cDNA, consistent with the conclusion that these polypeptides have not been modified by proteolytic processing in vivo or in vitro (Sakurai et al., 1995). Smaller polypeptides recognized by anti-CNA3 and anti–NBI-2 may have been proteolytically modified in vitro despite extensive precautions to prevent it. The observation of multiple polypeptides with molecular masses of ⩾190 kD for both BI and rbA is consistent with extensive alternative splicing of both isoforms of α_{1A}.

Pharmacologically Distinct Isoforms of α_{1A} in Rat Brain

The rbA and BI isoforms of α_{1A} have similar functional and pharmacological properties when expressed in *Xenopus* oocytes (Sather et al., 1993; Stea et al., 1994). However, immunoprecipitation of these isoforms from brain and analysis of their neurotoxin-binding properties have revealed pharmacological differences. Our pharmacological experiments using radioactive ligands demonstrated that anti-CNA3, anti–NBI-1, and anti–NBI-2 antibodies
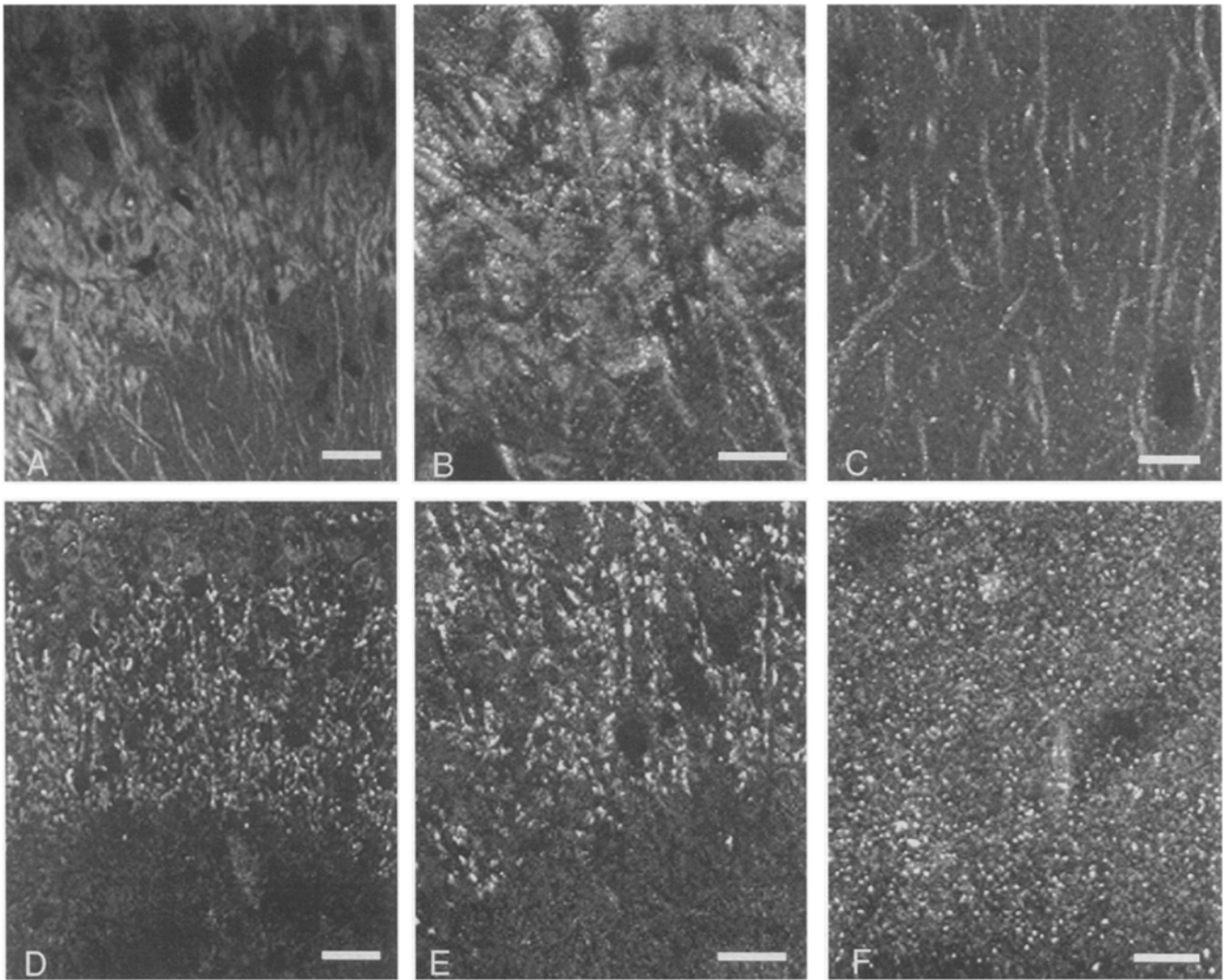
Figure 10. Distribution of rbA and BI isoforms of α_{1A} in the CA3 region of the hippocampus. Tissue sections of adult rat brain stained with anti-CNA3 or anti–NB1-2 antibodies using the immunofluorescence technique as described in Materials and Methods. (*A*) Low magnification of anti–NB1-2, illustrating staining of cell bodies and dendrites. (*B*) Higher magnification of staining of NB1-2 along the proximal dendrites of CA3 neurons, with occasional staining of punctate structures. (*C*) Staining of anti–NB1-2 along the distal dendrites of CA3 pyramidal neurons, with occasional staining of punctate structures along dendritic surfaces. (*D*) Tissue section stained with anti-CNA3, illustrating the low level of staining of the CA3 pyramidal cell soma and dense staining of punctate synaptic structures. (*E*) Tissue section stained with anti-CNA3, demonstrating the staining of mossy fiber terminals forming synapses on the proximal dendrites of CA3 pyramidal neurons. (*F*) Higher magnification of tissue stained with anti-CNA3, showing the staining of punctate structures in the region where the distal dendrites of CA3 pyramidal neurons reside. Bars: (*A*, *D*, and *G*) 50 μm; (*B*, *C*, *E*, *F*, *H*, and *I*) 25 μm.

do not immunoprecipitate either dihydropyridine or ω-cono-toxin GVIA binding sites, but specifically immunoprecipitate high affinity ω-conotoxin MVIIC receptor sites. [^{125}I]ω-conotoxin MVIIC receptors immunoprecipitated with anti-CNA3 contain a high affinity site for ω-conotoxin MVIIC with IC$_{50}$ of 100 pM, whereas [^{125}I]ω-conotoxin MVIIC receptors immunoprecipitated with anti–NBI-2 contain two binding sites with distinct affinities for ω-conotoxin MVIIC (IC$_{50}$ of ~100 pM and ~1 μM). High affinity ω-conotoxin MVIIC receptor sites recognized by anti-CNA3 and anti–NBI-2 are consistent with the conclusion that α_{1A} forms Q-type calcium channels because ω-conotoxin MVIIC blocks α_{1A} currents expressed in *Xenopus* oocytes and Q-type

currents in the cerebellar granule neurons with IC$_{50}$ < 150 nM (Sather et al., 1993; Stea et al., 1994; Zhang et al., 1993; Randall and Tsien, 1995). In contrast, native P-type calcium currents recorded in cerebellar Purkinje cells are blocked by higher concentrations of ω-conotoxin MVIIC (IC$_{50}$ of 1–10 μM; Hillyard et al., 1992). Several lines of evidence suggest that both Q-type and P-type calcium channels may contain α_{1A} subunits. (*a*) P/Q-type calcium channels are dihydropyridine- and ω-conotoxin GVIA–resistant (Llinas et al., 1989; Sather et al., 1993; Stea et al., 1994). (*b*) α_{1A} transcripts are expressed in cells with P-type and Q-type calcium channels (Mori et al., 1991; Starr et al., 1991). (*c*) α_{1A} coexpressed with specific β subunits in *Xenopus* oo-
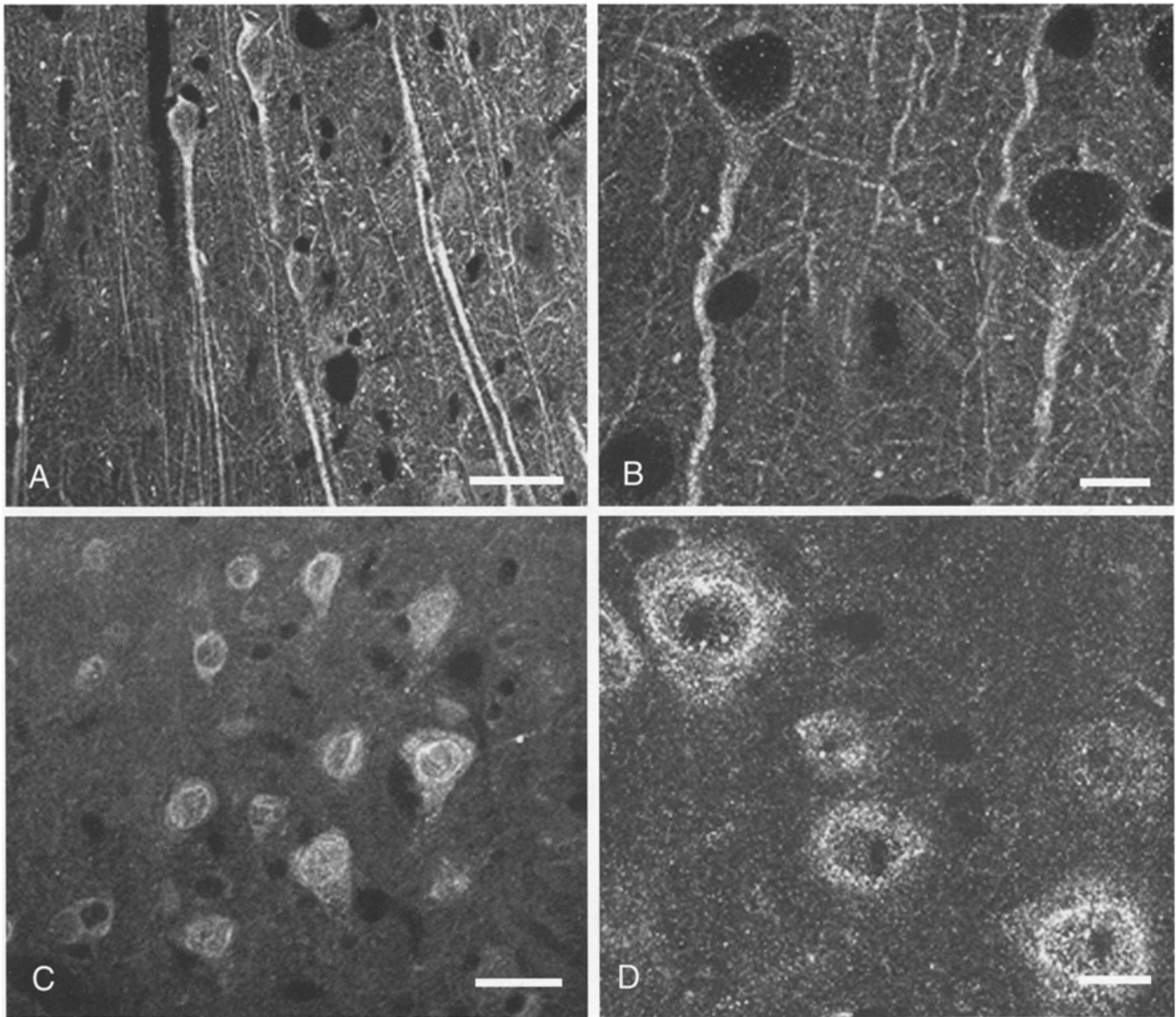
Figure 11. Localization of α_{1A} isoforms in the dorsal cerebral cortex. Sagittal sections of adult rat brain were stained with anti-CNA3 or anti–NB1-2 using the immunofluorescence technique described in Materials and Methods. (*A*) Tissue section stained with anti–NB1-2, illustrating the dense staining along the entire length of the dendrites of neurons located throughout the dorsal cortex. (*B*) Higher magnification of anti–NB1-2 staining in the dorsal cortex, demonstrating both smooth dendritic staining and staining of occasional punctate structures superimposed upon the dendritic surface. (*C*) Tissue section incubated with anti-CNA3, showing low levels of staining associated with the cell bodies of neurons. (*D*) Higher magnification of anti-CNA3 staining, demonstrating immunoreactivity associated with cell bodies and in punctate structures in the surrounding neuropil. Bars: (*A*, *C*, and *E*) 50 μm; (*B*, *D*, and *F*) 25 μm.

cytes yields barium currents with kinetics similar to P-type currents (Stea et al., 1994; DeWaard and Campbell, 1995). (*d*) α_{1A} is localized in cell bodies, dendrites, and synapses where both P-type and Q-type calcium currents are measured (Ousley and Froehner, 1994; Westenbroek et al., 1993, 1995). Thus, the low affinity sites for ω-conotoxin MVIIC recognized by anti–NBI-2 (Fig. 4) may represent native P-type calcium channels that are encoded by alternatively spliced isoforms of α_{1A} mRNA and have distinct pharmacology. A definitive analysis of this point would require studies of the high affinity binding of ω-agatoxin IVA which distinguishes P-type and Q-type calcium channels (Randall and Tsien, 1995), but this ligand has proven

difficult to use for specific binding studies with immunoprecipitated α_{1A} in our hands, and neither rbA nor BI yields calcium channels with high affinity for ω-agatoxin IVA when expressed in *Xenopus* oocytes (Sather et al., 1993; Stea et al., 1994).

α_{1A} Subunits Interact with Proteins Involved in Synaptic Exocytosis

According to the soluble *N*-ethylmaleimide–sensitive (NSF) attachment protein receptor (SNARE) hypothesis of exocytosis (Söllner et al., 1993), synaptic vesicles interact with targets for fusion when NSF and a soluble NSF attachment

protein (SNAP) bind to membrane-associated SNARES that are present in the vesicle and target membranes (designated v- and t-SNAREs, respectively). In the nerve terminal, the v-SNARE is the synaptic vesicle-associated membrane protein VAMP/synaptobrevin (Baumert et al., 1989; Trimble et al., 1990) and the t-SNAREs are syntaxin (Bennett et al., 1992; Inoue et al., 1992; Yoshida et al., 1992), and SNAP25 (Oyler et al., 1989). All assemble with SNAPs and NSF into 20 S fusion particles, resulting in the tight docking of the synaptic vesicles at the active zones (Söllner et al., 1993; Calakos et al., 1994; for review see Jahn and Südhof, 1994). Neurotransmitter release is ultimately triggered by high cytoplasmic calcium concentrations of the order of 100 μM, suggesting that voltage-gated calcium channels are clustered in the active zone, docked close to synaptic vesicles (Llinas et al., 1992). Presynaptic N-type calcium channels are associated with syntaxin (Bennett et al., 1992; Yoshida et al., 1992; Lévèque et al., 1992, 1994), synaptobrevin/VAMP (El Far et al., 1995), and SNAP25 (Lévèque et al., 1994). Interaction with syntaxin and SNAP25 is mediated by a specific sequence in L_{II-III} (Sheng et al., 1994, 1996), and coexpression of syntaxin in Xenopus oocytes modulates the voltage dependence of inactivation of calcium channels containing α_{1A} and α_{1B} (Bezprozvanny et al., 1995). Synaptotagmin, a calcium-binding protein of synaptic vesicles is also coimmunoprecipitated with syntaxin (Bennett et al., 1992; Yoshida et al., 1992), and is associated with N-type calcium channels (Lévèque et al., 1992, 1994; O'Conner et al., 1993). In contrast, class C L-type calcium channels are not associated with a synaptic vesicle fusion complex (Sheng et al., 1994; El Far et al., 1995). Our results with anti-CNA3 and anti–NBI-2 show that the rbA and BI isoforms of α_{1A} are associated with syntaxin and synaptotagmin in the rat brain, indicating that both α_{1A} subunit isoforms are involved in synaptic exocytosis at presynaptic nerve terminals. Direct, calcium-dependent interaction of a synaptic protein interaction site in the first half of L_{II-III} of α_{1B} and of the BI isoform of α_{1A} with syntaxin and SNAP25 has been observed in binding assays in vitro (Sheng et al., 1996; Rettig et al., 1996). However, the corresponding part of L_{II-III} of rbA binds SNAP25 but not syntaxin (Rettig et al., 1996), suggesting that a structural difference in L_{II-III}, which results from alternative RNA splicing, causes differential binding affinity for syntaxin.

An SDS-resistant complex consisting of syntaxin, SNAP25, and VAMP/synaptobrevin has been characterized in previous work (Hayashi et al., 1994; Chapmann et al., 1994; McMahon and Südhof, 1995). In our experiments, α_{1A} subunits recognized by anti-CNA3 were specifically associated with syntaxin in an SDS-resistant complex that was stable to incubation at 50–55°C for 30 min. Synaptotagmin was associated with this complex, but its association was not SDS resistant. Our results that α_{1A} and α_{1B} subunits of presynaptic calcum channels are specifically associated with the SDS-resistant core complex support a central role for this complex in docking and exocytosis of synaptic vesicles.

Differential Localization of the rbA and BI Isoforms of α_{1A}

In a previous study, we have shown that calcium channels

containing α_{1A} subunits recognized by the broad specificity antibody anti-CNA1 are present in low density on dendrites and some cell bodies, and are concentrated at approximately eightfold higher density in presynaptic terminals making synapses on cell bodies and on dendritic shafts and spines of many classes of neurons (Westenbroek et al., 1993, 1995). Class A calcium channels recognized by anti-CNA1 were especially prominent in the synapses of the parallel fibers of cerebellar granule cells on the dendrites of the Purkinje neurons, where their localization in presynaptic terminals was confirmed by double labeling with the synaptic membrane protein syntaxin or by microinjection of the postsynaptic marker Neurobiotin (Westenbroek et al., 1993, 1995). Anti-CNA1 staining represents the sum of the staining patterns that we observed with anti-CNA3 and anti-NB1-2 antibodies in these experiments. Similar staining of punctate structures was observed with anti-CNA3 and anti-NBI-2, indicating that both of these isoforms are present in nerve terminals. These immunocytochemical results are consistent with our immunoprecipitation experiments showing that both isoforms are associated with syntaxin and synaptotagmin. However, these isoform-specific antibodies also revealed differential distribution of the BI and rbA isoforms in both dendrites and nerve terminals.

The rbA isoform recognized by anti-CNA3 is localized predominantly in cell bodies and terminals. In contrast, the BI isoform recognized by anti–NBI-2 is located along the surface of dendrites as well as in cell bodies and nerve terminals in the cerebellum, hippocampus, and cerebral cortex. These results indicate that the BI and rbA isoforms, which are specifically recognized by these antibodies, contain different targeting information that specifies a difference in their localization in dendrites. This differential localization may also imply a functional difference for the BI and rbA isoforms of α_{1A}. Previous studies have suggested that the dendrites of cerebellar Purkinje neurons are important sites of calcium entry (Llinas and Sugimori, 1980; Tank et al., 1988), as are the dendrites of hippocampal pyramidal neurons (Regehr et al., 1989). Increases in intracellular calcium in cerebellar Purkinje dendrites evoked by brief pulses of high K^+ are blocked by low concentrations of ω-agatoxin IVA, while ω-conotoxin GVIA and ω-conotoxin MVIIC block only a small fraction of the intracellular calcium rise (Bindokas et al., 1993). This suggests that P-type calcium channels, which are highly sensitive to ω-agatoxin IVA, are located in Purkinje cell dendrites in high density, and, to a lesser extent, N-type and Q-type calcium channels are also present. It is possible that our anti-NBI-2 antibody recognizes the BI isoform that is localized in dendrites and forms P-type calcium channels. In contrast, the rbA isoform recognized by anti-CNA3 appears to be localized preferentially in the cell body of neurons. Localization in the cell body appears to be both cytoplasmic as well as on the cell surface. The cytoplasmic staining may represent α_{1A} subunits that are targeted for transport to the nerve terminals. Overall, our localization studies suggest that the different isoforms of the α_{1A} subunit have both differential and overlapping distributions along the cell bodies and dendrites of central neurons, which may position them for cell type–specific roles in integration and propagation of excitatory synaptic signals.

In many regions, such as the granule cell layer and distal

dendritic fields of the molecular layer of the cerebellum, the pattern of staining of nerve terminals with anti–NBI-2 and anti-CNA3 appears identical. The presence of more than one isoform of α_{1A} in a single nerve terminal may allow these channels to fine tune the voltage dependence, timing, or regulation of calcium influx, which in turn is used to control the timing and extent of secretion of fast neurotransmitters and/or neuropeptides. Distinct differences in the staining of nerve terminals by these isoform-specific antibodies were also observed. The rbA isoform recognized by anti-CNA3 is present at high concentration in the mossy fiber terminals on the proximal region of the dendrites of CA3 pyramidal neurons and in nerve terminals forming synapses on the distal dendrites of CA3 neurons (Fig. 10, D–F), while the BI isoform recognized by anti–NBI-1 is absent or present at very low levels in a small subset of these terminals (Fig. 10, A–C). These results are also consistent with the idea that the rbA isoform is a component of P-type calcium channels, since transmission at the mossy fiber synapse is highly sensitive to ω-agatoxin IVA (Castillo et al., 1994).

Anti-CNA3 antibodies stain a smaller fraction of nerve terminals on the dendrites of Purkinje neurons than anti–NBI-2 (Fig. 7, A–D), and nerve terminals stained by anti–CNA3 are sometimes organized in a linear array along proximal dendrites in a pattern reminiscent of the climbing fibers, while this pattern is not observed for anti–NBI-2 antibodies. These results suggest differential localization of the BI and rbA isoforms in the nerve terminals of the parallel fibers of the granule cells, which contribute the majority of synaptic input to the Purkinje neurons, and in the nerve terminals of the climbing fibers, which contribute a smaller portion of the synaptic input. Differential localization of rbA and BI isoforms in synapses in the hippocampus and cerebellum may indicate a functional specialization of different isoforms of class A calcium channels in mediating synaptic transmission at different synapses.

References

Baumert, M., P.R. Maycox, F. Navone, P. De Camilli, and R. Jahn. 1989. Synaptobrevin: an integral membrane protein of 18,000 daltons present in small synaptic vesicle of rat brain. EMBO (Eur. Mol. Biol. Organ.) J. 8:379–384.

Bennett, M.K., N. Calakos, and R.H. Scheller. 1992. Syntaxin: a synaptic protein implicated in docking of synaptic vesicles at presynaptic active zones. Science (Wash. DC). 257:255–259.

Bezprozvanny, I., R.H. Scheller, and R.W. Tsien. 1995. Functional impact of syntaxin on gating of N-type and Q-type calcium channels. Nature (Lond.). 378:623–626.

Bindokas, V.P., J.R. Brorson, and R.J. Miller. 1993. Characteristics of voltage-sensitive calcium channels in dendrites of cultured rat cerebellar neurons. Neuropharmacol. 32:1213–1220.

Birnbaumer, L., K.P. Campbell, W.A. Catterall, M.M. Harpold, F. Hofmann, W.A. Horne, Y. Mori, A. Schwartz, T.P. Snutch, T. Tanabe et al. 1994. The naming of voltage-gated Ca^{2+} channels. Neuron. 13:505–506.

Bowersox, S.S., G.P. Miljanich, Y. Sugiura, C. Li, L. Nadasdi, B.B. Hoffman, J. Ramachandran, and C.-P. Ko. 1995. Differential blockade of voltage-sensitive calcium channels at the mouse neuromuscular junction by novel ω-conopeptides and ω-agatoxin IVA. J. Pharmacol. Exp. Ther. 273:248–256.

Calakos, N., M.K. Bennett, K. Peterson, and R.H. Scheller. 1994. Protein-protein interactions contributing to the specificity of intracellular vesicular trafficking. Science (Wash. DC). 263:1146–1149.

Castillo, P.E., M.G. Weisskopf, and R.A. Nicoll. 1994. The role of Ca^{2+} channels in hippocampal mossy fiber synaptic transmission and long-term potentiation. Neuron. 12:261–269.

Catterall, W.A. 1988. Structure and function of voltage-sensitive ion channels. Science (Wash. DC). 242:50–61.

Chapmann, E.R., S. An, N. Barton, and R. Jahn. 1994. SNAP-25, a t-SNARE which binds to both syntaxin and synaptobrevin via domains may form coiled coils. J. Biol. Chem. 269:27427–27432.

DeWaard, M.D., and K.P. Campbell. 1995. Subunit regulation of the neuronal α_{1A} Ca^{2+} channel expressed in Xenopus oocytes. J. Physiol. 485:619–634.

Dubel, S.J., T.V.B. Starr, J. Hell, M.K. Ahlijanian, J.J. Enyeart, W.A. Catterall, and T.P. Snutch. 1992. Molecular cloning of the α1 subunit of an ω-conotoxin-sensitive calcium channel. Proc. Natl. Acad. Sci. USA. 89:5058–5062.

Dunlap, K., J.I. Luebke, and T.J. Turner. 1995. Exocytotic Ca^{2+} channels in mammalian central neurons. Trends Neurosci. 18:89–98.

El Far, O., N. Charvin, C. Leveque, N. Martin-Moutot, M. Takahashi, and M.J. Seagar. 1995. Interaction of a synaptobrevin (VAMP)-syntaxin complex with presynaptic calcium channels. FEBS Lett. 361:101–105.

Fujita, Y., M. Mynlieff, R.T. Dirksen, M.S. Kim, T. Niidome, J. Nakai, T. Freidrich, N. Iwabe, T. Miyata, T. Furuichi et al. 1993. Primary structure and functional expression of the ω-conotoxin-sensitive N-type calcium channel from rabbit brain. Neuron. 10:585–598.

Gordon, D., D. Merrick, D.A. Wollner, and W.A. Catterall. 1988. Biochemical properties of sodium channels in a wide range of excitable tissues studied with site-directed antibodies. Biochemistry. 27:7032–7038.

Hayashi, T., H. McMahon, S. Yamazaki, T. Binz, Y. Hata, T.C. Südhof, and H. Niemann. 1994. Synaptic vesicle membrane fusion complex: action of clostridial neurotoxins on assembly. EMBO (Eur. Mol. Biol. Organ.) J. 13: 5051–5061.

Hell, J.W., R.E. Westenbroek, C. Warner, M.K. Ahlijanian, W. Prystay, M.M. Gilbert, T.P. Snutch, and W.A. Catterall. 1993. Identification and differential subcellular localization of the neuronal class C and class D L-type calcium channel α1 subunits. J. Cell Biol. 123:949–961.

Hillyard, D.R., V.D. Monje, I.M. Mintz, B.P. Bean, L. Nadasdi, J. Ramachandran, G. Miljanich, A. Azimi-Zoonooz, J.M. McIntosh, L.J. Cruz et al. 1992. A new conus peptide ligand for mammalian presynaptic Ca^{2+} channels. Neuron. 9:69–77.

Horne, A.L., and J.A. Kemp. 1991. The effect of ω-conotoxin GVIA on synaptic transmission within the nucleus accumbens and hippocampus of the rat in vitro. Br. J. Pharmacol. 103:1733–1739.

Inoue, A., K. Obata, and K. Akagawa. 1992. Cloning and sequence analysis of cDNA for a neuronal cell membrane antigen, HPC-1. J. Biol. Chem. 267: 10613–10619.

Isom, L.L., K.S. DeJongh, and W.A. Catterall. 1994. Auxiliary subunits of voltage-gated ion channels. Neuron. 12:1183–1194.

Jahn, R., and T.C. Südhof. 1994. Synaptic vesicles and exocytosis. Annu. Rev. Neurosci. 17:219–246.

Lévèque, C., T. Hoshino, P. David, Y. Shoji-Kasai, K. Leye, A. Omori, B. Lang, O. El Far, K. Sato, N. Martin-Moutot et al. 1992. The synaptic vesicle protein synaptotagmin associates with Ca^{2+} channels and is a putative Lambert-Eaton myasthenic syndrome antigen. Proc. Natl. Acad. Sci. USA. 89:3625–3629.

Lévèque, C., O. El Far, N. Martin-Moutot, K. Sato, R. Kato, M. Takahashi, and M.J. Seagar. 1994. Purification of the N-type calcium channel in association with syntaxin and synaptotagmin. A complex implicated in synaptic vesicle exocytosis. J. Biol. Chem. 269:6306–6312.

Llinas, R., and M. Sugimori. 1980. The electrophysiological properties of in vitro Purkinje cell dendrites in mammalian cerebellar slices. J. Physiol. 305: 197–213.

Llinas, R., M. Sugimori, J.-W. Lin, and B. Cherksey. 1989. Blocking and isolation of a Ca^{2+} channel from neurons in mammals and cephalopods utilizing a toxin fraction (FTX) from funnel web spider venom. Proc. Natl. Acad. Sci. USA. 86:1689–1693.

Llinas, R., M. Sugimori, and R.B. Silver. 1992. Microdomains of high calcium concentration in a presynaptic terminal. Science (Wash. DC). 256:677–679.

Luebke, J.P., K. Dunlap, and T. Turner. 1993. Multiple calcium channel types control glutamatergic synaptic transmission in the hippocampus. Neuron. 11: 895–902.

Matthew, W.D., L. Tsavaler, and L.F. Reichardt. 1981. Identification of a synaptic vesicle-specific membrane protein with a wide distribution in neuronal and neurosecretory tissue. J. Cell Biol. 91:257–269.

McLean, I.W., and P. Nakane. 1974. Periodate-lysine-paraformaldehyde fixative for immunoelectron microscopy. J. Histochem Cytochem. 22:1077–1083.

McMahon, H.T., and T.C. Südhof. 1995. Synaptic core complex of synaptobrevin, syntaxin, and SNAP25 forms high affinity α-SNAP binding site. *J. Biol. Chem.* 270:2213–2217.

Merrifield, R.B. 1963. Solid phase peptide synthesis I. The synthesis of a tetra peptide. *J. Am. Chem. Soc.* 85:2149–2154.

Mori, Y., T. Friedrich, M.S. Kim, A. Mikami, J. Nakai, P. Ruth, E. Broose, F. Hofmann, V. Flockerzi, T. Furuichi et al. 1991. Primary structure and functional expression from complementary DNA of a brain calcium channel. *Nature (Lond.).* 350:398–402.

O'Conner, V.M., O. Shamotienko, E. Grishin, and H. Betz. 1993. On the structure of the 'synaptosecretosome'. *FEBS Lett.* 326:255–260.

Olivera, B.M., G.P. Miljanich, J. Ramachandran, and M.E. Adams. 1994. Calcium channel diversity and neurotransmitter release: the ω-conotoxins and ω-agatoxins. *Annu. Rev. Biochem.* 63:823–867.

Ousley, A.H., and S.C. Froehner. 1994. An anti-peptide antibody specific for the class A calcium channel α1 subunit labels mammalian neuromuscular junction. *Proc. Natl. Acad. Sci. USA.* 91:12263–12267.

Oyler, G.A., G.A. Higgins, R.A. Hart, E. Battenberg, M. Billigsley, F.E. Bloom, and M.C. Wilson. 1989. The identification of a novel synaptosomal-associated protein, SNAP-25, differentially expressed by neuronal subpopulations. *J. Cell Biol.* 109:3039–3052.

Posnett, D.M., H. McGrath, and J.P. Tam. 1988. A novel method for producing anti-peptide antibodies. Production of site-specific antibodies to the T cell antigen receptor beta-chain. *J. Biol. Chem.* 263:1719–1725.

Randall, A., and R.W. Tsien. 1995. Pharmacological dissection of multiple types of Ca^{2+} channel currents in rat cerebellar granule neurons. *J. Neurosci.* 15:2995–3012.

Regehr, W.G., and I.M. Mintz. 1994. Participation of multiple calcium channel types in transmission at single climbing fiber to Purkinje cell synapses. *Neuron.* 12:605–613.

Regehr, W.G., J.A. Connor, and D.W. Tank. 1989. Optical imaging of calcium accumulation in hippocampal pyramidal cells during synaptic activation. *Nature (Lond.).* 341:533–536.

Rettig, J., Z.H. Sheng, D.K. Kim, C.D. Hodson, T.P. Snutch, and W.A. Catterall. 1996. Isoform-specific interaction of the α$_{1A}$ subunits of brain Ca^{2+} channels with the presynaptic proteins syntaxin and SNAP-25. *Proc. Natl. Acad. Sci. USA.* In press.

Sakamoto, J., and K.P. Campbell. 1991. A monoclonal antibody to the β subunit of the skeletal muscle dihydropyridine receptor immunoprecipitates the brain ω-conotoxin GVIA receptor. *J. Biol. Chem.* 266:18914–18919.

Sakurai, T., J.W. Hell, A. Woppmann, G.P. Miljanich, and W.A. Catterall. 1995. Immunochemical identification and differential phosphorylation of alternatively spliced forms of the α$_{1A}$ subunit of brain calcium channels. *J. Biol. Chem.* 270:21234–21242.

Sather, W.A., T. Tanabe, J.-F. Zhang, Y. Mori, M.A. Adams, and R.W. Tsien. 1993. Distinctive biophysical and pharmacological properties of class A (BI) calcium channel α1 subunits. *Neuron.* 11:291–303.

Sheng, Z.-H., J. Rettig, M. Takahashi, and W.A. Catterall. 1994. Identification of a syntaxin-binding site on N-type calcium channels. *Neuron.* 13:1303–1313.

Sheng, Z.-H., J. Rettig, T. Cook, and W.A. Catterall. 1996. Calcium-dependent interaction of N-type calcium channels with the synaptic core complex. *Nature (Lond.).* 379:451–454.

Smith, D.B., and K.S. Johnson. 1988. Single-step purification of polypeptides expressed in *Escherichia coli* as fusion with glutathione *S*-transferase. *Gene (Amst.).* 67:31–40.

Snutch, T.P., and P.B. Reiner. 1992. Ca^{2+} channels: diversity of form and function. *Curr. Opin. Neurobiol.* 2:247–253.

Snutch, T.P., J.P. Leonard, M.M. Gilbert, H.A. Lester, and N. Davidson. 1990.

Rat brain expresses a heterogeneous family of calcium channels. *Proc. Natl. Acad. Sci. USA.* 87:3391–3395.

Söllner, T., M.K. Bennett, S.W. Whiteheart, R.H. Scheller, and J.E. Rothman. 1993. A protein assembly-disassembly pathway in vitro that may correspond to sequential steps of synaptic vesicle docking, activation, and fusion. *Cell.* 75:409–418.

Soong, T.W., E. Bourinet, S. Slaymaker, E. Matthew, S.J. Dubel, S.R. Vincent, and T.P. Snutch. 1994. Alternative splicing generates rat brain α$_{1A}$ calcium channel isoforms with distinct electrophysiological properties. *Soc. Neurosci. Abstr.* 20:70.

Starr, T.V.B., W. Prystay, and T.P. Snutch. 1991. Primary structure of a calcium channel that is highly expressed in the rat cerebellum. *Proc. Natl. Acad. Sci. USA.* 88:5621–5625.

Stea, A., W.J. Tomlinson, T.W. Soong, E. Bourinet, S.J. Dubel, S.R. Vincent, and T.P. Snutch. 1994. Localization and functional properties of a rat brain α$_{1A}$ calcium channel reflect similarities to neuronal Q- and P-type channels. *Proc. Natl. Acad. Sci. USA.* 91:10576–10580.

Takahashi, T., and A. Momiyama. 1993. Different types of calcium channels mediate central synaptic transmission. *Nature (Lond.).* 366:156–158.

Tank, D.W., M. Sugimori, J.A. Connor, and R.R. Llinas. 1988. Spatially resolved calcium dynamics of mammalian Purkinje cells in cerebellar slices. *Science (Wash. DC).* 242:773–777.

Trimble, W.S., T.S. Gray, L.A. Elferink, M.C. Wilson, and R.H. Scheller. 1990. Distinct patterns of expression of two VAMP genes within the rat brain. *J. Neurosci.* 10:1380–1387.

Uchitel, O.D., D.A. Protti, V. Sanchez, B.D. Cherksey, M. Sugimori, and R. Llinas. 1992. P-type voltage-gated calcium channel mediates presynaptic calcium influx and transmitter release in mammalian synapses. *Proc. Natl. Acad. Sci. USA.* 898:3330–3333.

West, J.W., R. Numann, B.J. Murphy, T. Scheuer, and W.A. Catterall. 1991. A phosphorylation site in the Na$^+$ channel required for modulation by protein kinase C. *Science (Wash. DC).* 254:866–868.

Westenbroek, R.E., J.W. Hell, C. Warner, S.J. Dubel, T.P. Snutch, and W.A. Catterall. 1992. Biochemical properties and subcellular distribution of an N-type calcium channel α1 subunit. *Neuron.* 9:1099–1115.

Westenbroek, R.E., J.W. Hell, T. Sakurai, T.P. Snutch, and W.A. Catterall. 1993. Immunocytochemical localization of class A calcium channels in adult rat brain. *Soc. Neurosci. Abstr.* 19:1334.

Westenbroek, R.E., T. Sakurai, E.M. Elliott, J.W. Hell, T.V.B. Starr, T.P. Snutch, and W.A. Catterall. 1995. Immunochemical identification and subcellular distribution of the α$_{1A}$ subunits of brain calcium channels. *J. Neurosci.* 15:6403–6418.

Wheeler, D.B., A. Randall, and R.W. Tsien. 1994. Roles of N-type and Q-type Ca^{2+} channels in supporting hippocampal synaptic transmission. *Science (Wash. DC).* 264:107–111.

Williams, M.E., P.F. Brust, D.H. Feldman, S. Patthi, S. Simerson, A. Maroufi, A.F. McCue, G. Velicelebi, S.B. Ellis, and M.M. Harpold. 1992. Structure and functional expression of an ω-contoxin-sensitive human N-type calcium channel. *Science (Wash. DC).* 257:389–395.

Wu, L.-G., and P. Saggau. 1994. Adenosine inhibits evoked synaptic transmission primarily by reducing presynaptic calcium influx in area CA1 of hippocampus. *Neuron.* 12:1139–1148.

Yoshida, A., C. Oho, A. Omori, R. Kumakura, T. Ito, and M. Takahashi. 1992. HPC-1 is associated with synaptotagmin and ω-conotoxin receptor. *J. Biol. Chem.* 267:24925–24928.

Zhang, J.K., A.D. Randall, P.T. Ellinor, W.A. Horne, W.A. Sather, T. Tanabe, T.L. Schwarz, and R.W. Tsien. 1993. Distinctive pharmacology and kinetics of cloned neuronal Ca^{2+} channels and their possible counterparts in mammalian CNS neurons. *Neuropharmacology.* 32:1075–1088.